NAVWEPS REPORT 8738
NOTS TP 3799
COPY 57

HITAB-BWSS PAYLOADS

by

John A. Hoyem, James E. Hurtt, and
Larry N. Pace
Astrometrics Division
Weapons Development Department

ABSTRACT. The objective of the HITAB program, under sponsorship of the Advanced Research Projects Agency (ARPA), was that of measuring certain infrared and ultraviolet characteristics of in-flight ballistic missile plumes, and of selected earth backgrounds. The measurements were obtained from instrumented high-altitude rocket probes.

This report documents the HITAB-BWSS payloads, which were designed to measure the Wiener spectrum of the earth's background in several narrow regions of the infrared. Experiment description, mission profile, vehicle-payload configuration, optics, optical calibration, and a resumé of the rocket flights are presented.

U.S. NAVAL ORDNANCE TEST STATION

China Lake, California

August 1965

U. S. NAVAL ORDNANCE TEST STATION

AN ACTIVITY OF THE BUREAU OF NAVAL WEAPONS

J. I. HARDY, CAPT., USN
Commander

WM. B. MCLEAN, PH.D.
Technical Director

FOREWORD

The HITAB program was conducted at the U.S. Naval Ordnance Test Station (NOTS) under sponsorship of the Advanced Research Projects Agency (ARPA), Department of Defense. This program was one of the several related research projects being conducted under the project title TABSTONE. Project TABSTONE represents one element of Project DEFENDER, which is administered by ARPA.

The objective of the HITAB program was to measure certain infrared and ultraviolet characteristics of in-flight ballistic missiles, and of earth backgrounds. These measurements are obtained from high-altitude rocket probes.

This program is specified in Advanced Research Projects Agency Order 243-61 of 18 May 1961, and, in subsequent amendments, current authorization for BuWeps is documented in WepTask RT 7046-001/216-7/F619-06-004.

Review for technical accuracy was given by George A. Wilkins.

Released by
D. K. MOORE, Head
Astrometrics Division
21 May 1965

Under authority of
F. H. KNEMEYER, Head
Weapons Development Dept.

NOTS Technical Publication 3799
NAVWEPS Report 8738

Published by . . . . . Weapons Development Department
Manuscript 40/65-12
Collation . . . . . Cover, 21 leaves, abstract cards
First printing . . . . . 190 numbered copies
Security classification . . . . . UNCLASSIFIED

INTRODUCTION

The HITAB rocket probe program was conducted by the U.S. Naval Ordnance Test Station (NOTS), under sponsorship of the Advanced Research Projects Agency (ARPA) as a portion of Project DEFENDER. The purpose of this program is to measure the infrared and ultraviolet radiation of powered ICBM targets during the launching phase and of the earth's background from an observation point in space.

This report documents a series of rocket probes, assigned the acronym HITAB-BWSS, which were designed to measure the Wiener spectrum of the earth's background in several narrow intervals in the infrared portion of the spectrum.

Data obtained by the HITAB-BWSS payloads are to be presented separately in a joint report by NOTS and the Institute of Science and Technology (IST), University of Michigan. This report will concern itself, therefore, with presenting details of the HITAB-BWSS experiment, mission profile, vehicle-payload configuration, optics, optical calibration, and the rocket flights conducted.

I. EXPERIMENT DESCRIPTION

There are a number of means that can be used to study and describe infrared backgrounds. These include the infrared picture, the line-scan, the one-dimensional Wiener spectrum, and the two-dimensional Wiener spectrum. A good deal of conjecture exists as to which of these methods constitutes the most effective approach to background study. Because of the current inability to produce high quality IR pictures, such a method is almost immediately dropped from consideration. The line-scan technique has been employed widely, with varying degrees of success. However, if one's interest lies in the gross statistics of a given background (i.e., the physical arrangement of the radiance sources over large background regions), some rather strong arguments have been presented for utilizing the Wiener spectrum method.

Wessely[1] has defined and qualified the two-dimensional Wiener spectrum in the following manner. "The Wiener spectrum is a statistical description of the spatial distribution of the background radiance. Its importance lies in the fact that from a knowledge of the two-dimensional Wiener spectrum one can determine the rms response to clutter of any linear infrared system."

[1] Wessely, Harry W. "How to Make Wiener Spectrum Measurements", Laboratories for Applied Sciences, University of Chicago, Chicago, Illinois; 11 March 1960. (An informal report.)

Perhaps the most poignant question in regard to the earth's infrared background is whether it is a statistically predictable function, and therefore, whether some "average" picture of the background can be formulated. The goal of the HITAB-BWSS experiments was to generate data on the two-dimensional Wiener spectrum of the earth's infrared background, in order to provide an additional test of the Wiener spectrum method. Data were to be obtained from a near-space viewing position, using instrumented sounding rocket payloads. Measurements were to be conducted simultaneously in several relatively narrow regions of the near-middle infrared spectrum to allow evaluation of the dependence upon wavelength.

THEORY

By a simple extension of one-dimensional Wiener spectrum techniques, two-dimensional data can be obtained. A straight-forward approach to the one-dimensional measurement will be outlined first, then expanded to cover the two-dimensional case.

What, first of all, does the term "Wiener spectrum" imply? Basically, the Wiener spectrum is the power spectrum of the function N(k), which is the distribution of background radiance with spatial wavenumber. R. Clark Jones[2] has coined the term Wiener spectrum in honor of Norbert Wiener, who developed the mathematical concepts used in the technique[3]. When reference is made to a one-dimensional spectrum, it refers to the power spectrum of the background distribution as measured along a single direction in the background. A two-dimensional spectrum is one obtained for two perpendicular directions in the distribution.

[2]Jones, R. Clark. "New Method of Describing and Measuring the Granularity of Photographic Materials", J OP SOC AM, Vol. 45, No. 10 (October, 1955), pp. 799 - 808.

[3]Wiener, Norbert. Acta Mathematica, Vol. 55 (1930) (Stockholm), pp. 117 - 258.

If one attempts to measure the one-dimensional Wiener spectrum of a background with a linear scan system, as both Jones and Wessely have shown, a radiometer with a rectangular view field is most appropriate[4, 5]. Such a view field is shown in Fig. 1, as it would appear projected upon a cluttered background scene. The scan is made in the direction normal to the long side of the field. In order to show the operation of such a radiometer, it is necessary to consider certain of its characteristics.

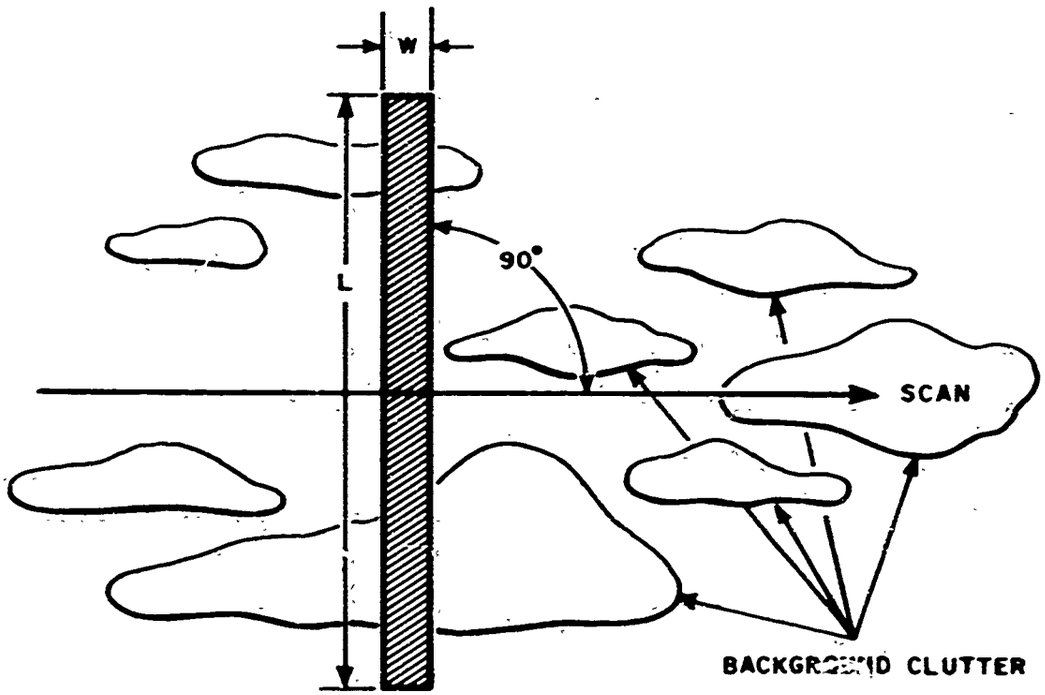

FIG. 1. Rectangular View Projected Upon a Cluttered Background Scene.

[4] Jones, R. Clark. "The Study of IR Backgrounds by the Wiener Spectrum Method", 1959. (A compendium of Jones' theoretical work on sky noise compiled by the Infrared Laboratory of the Willow Run Laboratories, University of Michigan.)

[5] Wessely, Harry W. "How to Make Wiener Spectrum Measurements", Laboratories for Applied Sciences, University of Chicago, Chicago, Illinois, 11 March 1960. (An informal report.)

The radiometer would include the following components: collecting optics, optical filtering to define the spectral response of the system, a detector sensitive in this spectral region, a detector signal amplifier, and some form of data retrieval system. All of these components bear upon the nature of the signals obtained by the radiometer.

Scanning the view field across the background distribution yields the condition known as "object space modulation". Except for the case where the background is uniformly brilliant, radiant signals monitored at the detector will be time-variant. The rate at which they fluctuate is determined by the background distribution and the scan rate. The frequency of the signals[6] monitored is given by

$$f = sk \ ,$$

where f is the electrical frequency produced in the detector, s is the scanning speed, and k is the spatial wavenumber. The wavenumber can be defined either in terms of the angle subtended by a pair of sources at the radiometer, or in terms of the distance separating them in object space. In either case the separation is measured in the scan direction, and the wavenumber is given by

$$k = \theta^{-1} \ , \text{ or } k = d^{-1} \ ,$$

where θ and d represent the angle subtended and object space distance, respectively. The choice of wavenumber units depends upon whether the scan mode is constant in angular rate or in rate of change of position in object space.

Because of the frequency response characteristics of the radiometer system, not all the frequencies produced will be passed by the system. Superpositioning the frequency response characteristics of the individual system components will generally net a bandpass system frequency response. Thus, there will be a band of spatial wavenumbers to which the system will respond optimally from an electronic standpoint.

The fact that the view field does not resolve the background infinitely well also affects the system performance. If the field were infinitely narrow, the background would be infinitely resolvable. Resolution of the view field is determined by its spatial admittance function, which, for a symmetrical rectangular view field is given by

---

[6] Ibid.

$$U(k_1, k_2) = \frac{\sin \pi k_1 W}{\pi k_1 W} \cdot \frac{\sin \pi k_2 L}{\pi k_2 L} ,$$

where k_1 and k_2 are two orthogonal axes in wavenumber space, W is the width of the field and L is the length. The spatial wavenumber passband, which this function defines, can be symbolized as a rectangle in wavenumber space (Fig. 2). To maintain the sense of its orientation, bear in mind that the k_1 axis corresponds to the scan direction. In this light, it will be noted that the rectangular view field has a very narrow wavenumber passband along the normal to the scan direction. Thus, it is "detuned" to variations in radiance along this direction. This satisfies a basic requirement for the one-dimensional Wiener spectrum measurement--that the data gathered be generated for a single direction in object space. As the length of the view field is increased, the system becomes more and more insensitive to background structure in every direction except that along the scan. Similarly, as the width of the field is decreased, the system assumes a broader passband in the scan direction.

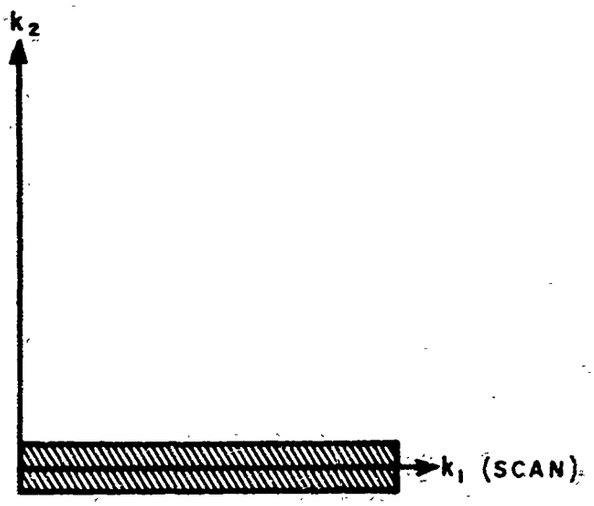

FIG. 2. Symbolized Spatial Wave Number Pass Band, Rectangular View Field.

The combination of view field and electrical frequency response characteristics yields the "spatio-temporal" admittance function of the system. Here the spatial aspects of the admittance derive from view

field characteristics, while the temporal aspects derive from system frequency response. The mean-squared response of a system to a given radiance distribution[7] is

$$\bar{V}^2 = C \int_{-\infty}^{\infty} \int_{-\infty}^{\infty} \left| Y(sk_1)\, U(k_1, k_2) \right|^2 N(k_1, k_2)\, dk_1 dk_2 ,$$

where $\bar{V}^2$ is the mean-squared output voltage, $Y(sk_1)$ is the temporal admittance, $U(k_1, k_2)$ is the spatial admittance, and $N(k_1, k_2)$ is the radiance distribution. Temporal admittance is expressed in terms of k_1 wavenumbers, since scanning is only done in the k_1 direction. The constant C accounts for detector responsivity, optical constants, and the like.

Assume that a given background distribution has been scanned with the one-dimensional measurement system. The output of the radiometer has been recorded with time on magnetic tape. It is necessary to know the "spatio-temporal" admittance function of the system, which can be represented as a rectangle in wavenumber space (Fig. 3). Given the scanning speed, the range of electrical frequencies corresponding to the spatial wavenumber bandpass of the system is defined. The raw data is submitted to a frequency analyzer, which is tuned to some frequency, f_a (corresponding to a spatial wavenumber $k_a = f_a/s$). Then the output of this filtering system is equal to the product of (1) the two-dimensional Wiener spectrum value at k_a, (2) the spatio-temporal admittance at k_a, (3) the radiometer constant C, and (4) the bandwidth of the frequency analyzer Δk. Since the last three of the four parameters are known, the one-dimensional Wiener spectrum at k_a is directly obtained. This process is carried out for the entire range of the spatial wavenumber passband, and yields the Wiener spectrum along the k_1 wavenumber axis.

[7] Jones, R. Clark. "New Method of Describing and Measuring the Granularity of Photographic Materials", J OP SOC AM, Vol. 45, No. 10 (October, 1955), pp. 799 - 808.

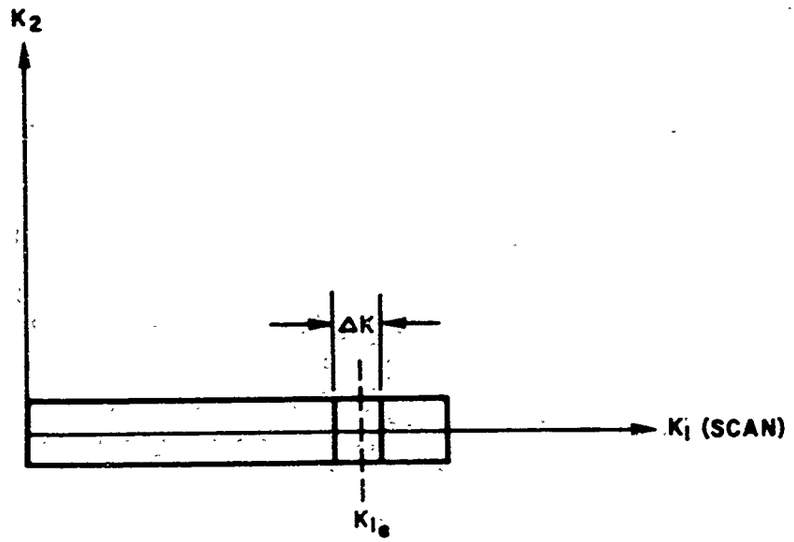

FIG. 3. Symbolized "Spatio-Temporal" Admittance Function.

Note that while a two-dimensional distribution is being scanned, the measurement confines itself to a single direction, because of the scan mode and the view field shape. The fact that the view field is not infinitely long means that the system does respond to variations along directions other than that of the scan. By making the view field length large with respect to the width, however, the contribution to the output by these off-axis variations is constrained to an insignificant level. Thus, the one-dimensional Wiener spectrum is obtained.

A simple extension of this technique will allow generation of rather coarse two-dimensional spectra. Here a pair of view fields are used, one normal to the scan direction, the other inclined to it. Figure 4 depicts the view field geometry. The normal view field is rectangular with its long dimension perpendicular to the scan line. The other is a parallelogram, inclined at 45 degrees to the normal element (labeled "inclined" element). Note that the widths of the two view fields are equal in the scan direction, and that the inclined field length is defined by projecting the normal field length onto the diagonal. In this manner, the two view fields scan the same background region, with the same spatial resolution in the scan direction.

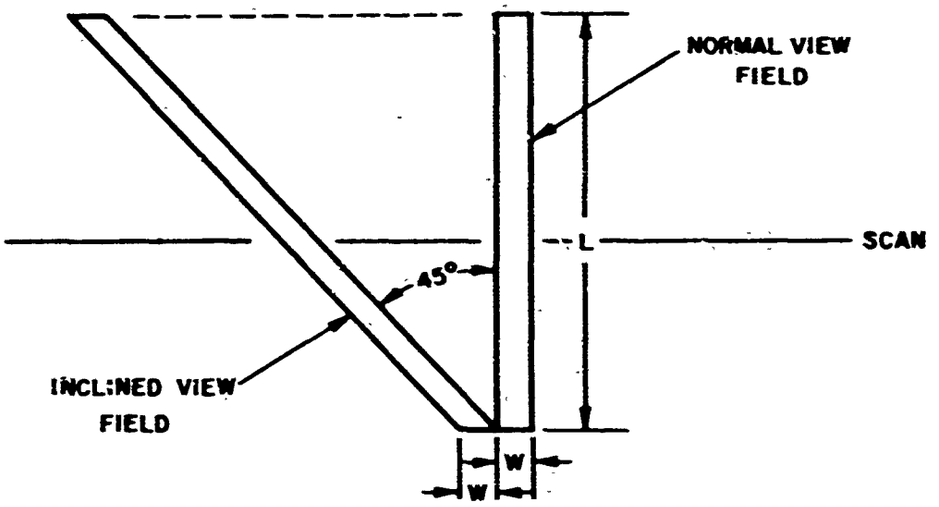

FIG. 4. Inclined View Fields.

The "spatio-temporal" admittance functions of these two radiometers follow the form encountered earlier, and can be symbolized in the same fashion (Fig. 5). Each radiometer's output from a given scan is analyzed as before, so that the values of the one-dimensional Wiener spectrum are determined along the scan and inclined directions in wavenumber space. The problem is to determine the one-dimensional Wiener spectrum along the axis normal to the scan (the k_2 axis). Extrapolation to the k_2 axis must be carried out in terms of wavenumber. To do this, one fixes the scalar magnitude of the vector wavenumber of interest, $|k|$, and determines the value of the Wiener spectrum for each sensor at the frequency corresponding to this wavenumber. Thus, for a wavenumber of interest $|k_2|=|k|$, one evaluates the normal sensor data at $k_{1_a}=|k|$, and the inclined sensor data at $k_{1_b}=\frac{\sqrt{2}|k|}{2}$ (Fig. 5). In this way, the values of the Wiener spectrum are determined at two points on the wavenumber arc of radius k. Extrapolation to the third point (on the k_2 axis) is then done on the basis of angular position in wavenumber space.

There is no question that this is a very coarse method. Extrapolation of a continuous function from just two points of that function is always a risky thing to attempt. One could improve upon the accuracy of the technique by using more sensors, inclined at other angles to the normal sensor. Practically this may not be possible.

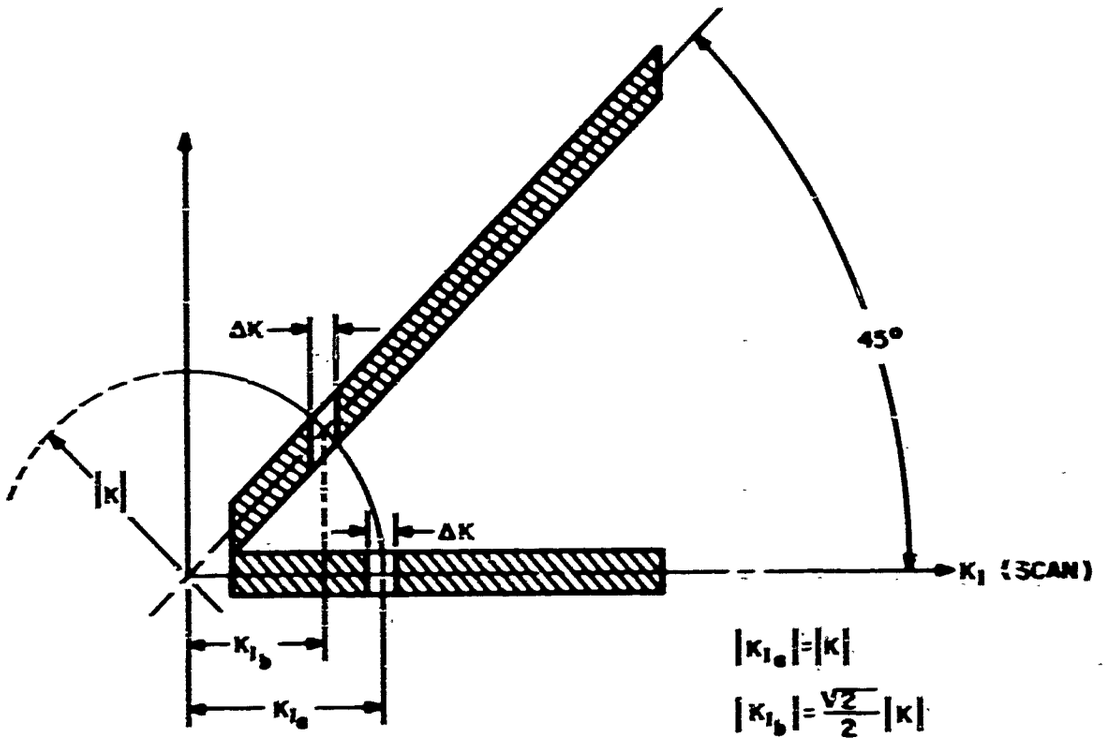

FIG. 5. Symbolized "Spatio-Temporal" Admittance Function (Inclined View Fields).

APPLICATION

Although there are other means to generate two-dimensional Wiener spectrum data than by the use of inclined view fields, it was decided to use this approach. This decision was based upon upon the nature of the payload-rocket system that was to be used, and upon the requirement for system simplicity.

As mentioned earlier, the two-dimensional Wiener spectrum measurements were to be conducted simultaneously in several regions of the infrared spectrum. Specific interest lay in those spectral regions for which the earth's atmosphere is either a very strong absorber or a very clear window. Hence, systems were designed to be sensitive at 2.2, 2.7, 3.8, and 4.3 microns. Because there was a need for wavelength correlation, every attempt was made to fit into each payload a two-element system for each of these spectral regions.

The HITAB-BWSS experiments employed a rocket system with which NOTS had considerable experience. This two-stage, solid-propellant system employed fin-induced spin for stability. The spinning motion of the vehicle was used to scan the radiometers across the background.

II. MISSION PROFILE

A two-stage, solid-propellant rocket system carried the HITAB-BWSS payloads aloft. An artist's conception of the mission is presented in Fig. 6. The rocket was launched at an angle of 84 degrees (or greater) above the horizontal, along a due South trajectory. The second-stage motor ignited 9.2 seconds after rocket launching. The second (final) stage of the motor burned for 6 seconds; so, 15 seconds after launching, the powered portion of flight was completed. At this time, the vehicle's speed was roughly 1.5 km/sec, and its velocity vector was approximately 82 degrees above the horizontal.

The optics carried aboard the payload were positioned so that their axes pointed aft, 30 degrees off the longitudinal axis of the vehicle. The pattern traced by these axes on the earth was a clockwise spiral. Only two sets of dual-field optics are shown in Fig. 6. Because of the bulk of the optical gear and associated equipment, it was not possible to fit four systems into each payload. Hence, each payload was fitted with two sets, one defined to respond in an atmospheric window, the other in an absorption region. Of the three payloads launched, all carried optics sensitive at 2.2 and 2.7 microns. More will be said about this aspect later.

By launching at 84 degrees elevation and by coasting between rocket stages, the payload was boosted to an altitude of roughly 140 kilometers at summit. A plot of altitude versus slant range is presented in Fig. 7. Attempts to track the BWSS vehicles with radar were unsuccessful during the entirety of the first two flights, and from launching to summit on the third. Therefore, theoretical trajectory data were scaled in terms of the meaningful data obtained on the third flight (from summit to impact) to produce this figure.

Requirements for cloud cover over the flight area were chosen in terms of the optical systems to be flown. Conditions were considered optimum if, in an area defined by an 80-km radius from the launching point, the cloud cover had a mean altitude of 7.6 km with 20 to 50 percent coverage. Naturally, such conditions would be heavily dependent upon the time of year. Even at the most promising times, the above requirements could not always be met. The final decision on cloud cover sufficiency was left to the NOTS representative in charge at the launching site. For studies within the intense absorption band at 2.7 microns, it was necessary that cloud tops be as high as possible to ensure favorable signal returns. Altitude considerations were not at all critical for the 2.2-micron region.

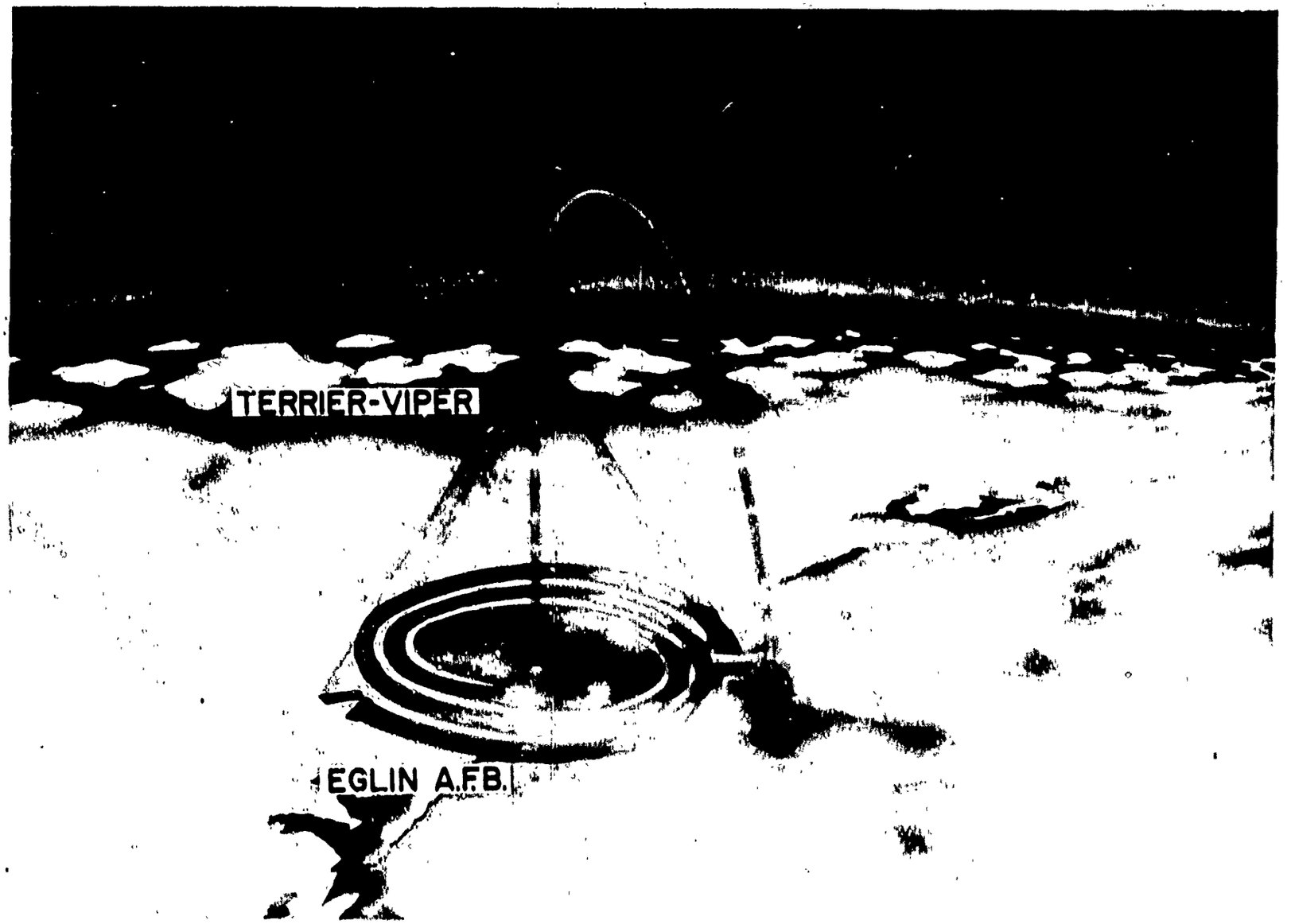

FIG. 6. HITAB-BWSS Mission Profile.

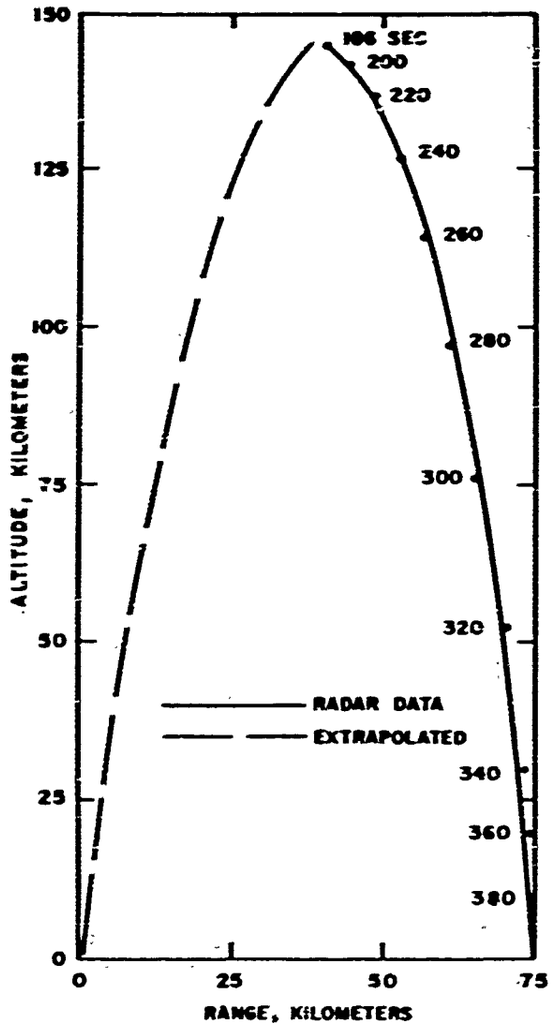

FIG. 7. HITAB-BWSS Altitude Versus Range Profile.

To provide optimum background illumination, launching was restricted to a window between 1000 and 1400 hours local time.

III. VEHICLE-PAYLOAD CONFIGURATION

Figure 8 shows the external configuration of the HITAB-BWSS rocket system. The first motor stage was a Terrier booster. A bell-shaped housing (labeled "Transition") coupled the first and second motor stages. This housing contained the necessary equipment to effect separation of the first-stage after burnout. Two detonators were positioned 180 degrees apart on a ring at the nose of the transition

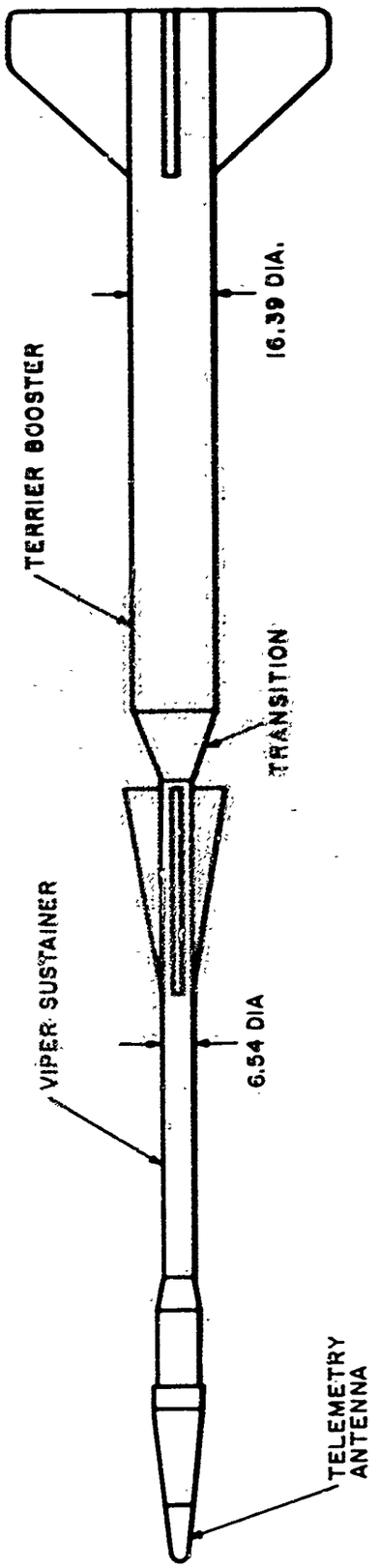

FIG. 8. External Configuration, HITAB-BWSS Rocket System.

piece. Actuation of these detonators fractured the ring, and decoupled the first stage from the remainder of the vehicle. Firing voltage was supplied to the detonators in the following manner. Motion of the vehicle at launching removed a pull wire from the transition section. This armed the separation mechanism. A deceleration switch was tripped when thrust from the first stage dropped below a preset value. The tripping of this switch initiated a short interval timer that applied firing voltage to the detonators a short time after thrust cutoff. This delay after thrust drop-off was necessary to ensure termination of all thrust from the engine; thus, guaranteeing that the separated motor would not overtake the coasting vehicle.

Vehicle spin rate during first-stage burning was held at a low value by the large moment of inertia about the longitudinal axis and the low velocity attained. During this period, the maximum spin rate achieved was approximately 1.5 rps. As soon as the first stage was separated, the moment of inertia decreased significantly, and the second-stage fins rapidly increased the spin rate to roughly 4 rps. Adjustment of fin cant angle for the first stage was done by rotating the entire fin. The effective cant angle of the second-stage fins was determined by tabs placed at their trailing edges. It was difficult to predict the resultant spin rate after first-stage separation. Experience showed that spin rates could vary from 2 to 10 rps. A spin rate of around 2 rps would be ideal from the data-gathering standpoint. Setting the second-stage fins to give this value on the average would have compromised system reliability.

The second-stage motor was a Viper 1C, manufactured by Lockheed Propulsion Corporation. It was fitted with an igniter, developed at NOTS, which was mounted at the head of the motor. Ignition of the second stage was effected by a mechanism carried in the payload. At launching, an acceleration switch in the payload was tripped by vehicle motion. The tripping of this switch started a timer that cycled for approximately 9 seconds before applying the necessary firing voltage to the igniter.

The payload was fitted with a threaded after-section that mated with a threaded section on the head of the second-stage motor. Each of the BWSS payloads varied slightly in configuration, although all three carried basically the same components. For convenience, the three payloads were assigned numeric identifications based upon their sequence of contruction (-01, -02, and -03). Variation between the layouts of the -01 and -02 payloads were slight. Figures 9 and 10 present views of the -02 and -03 payloads. The biggest single difference between these two payloads lay in the optical systems, which will be discussed in detail in this report.

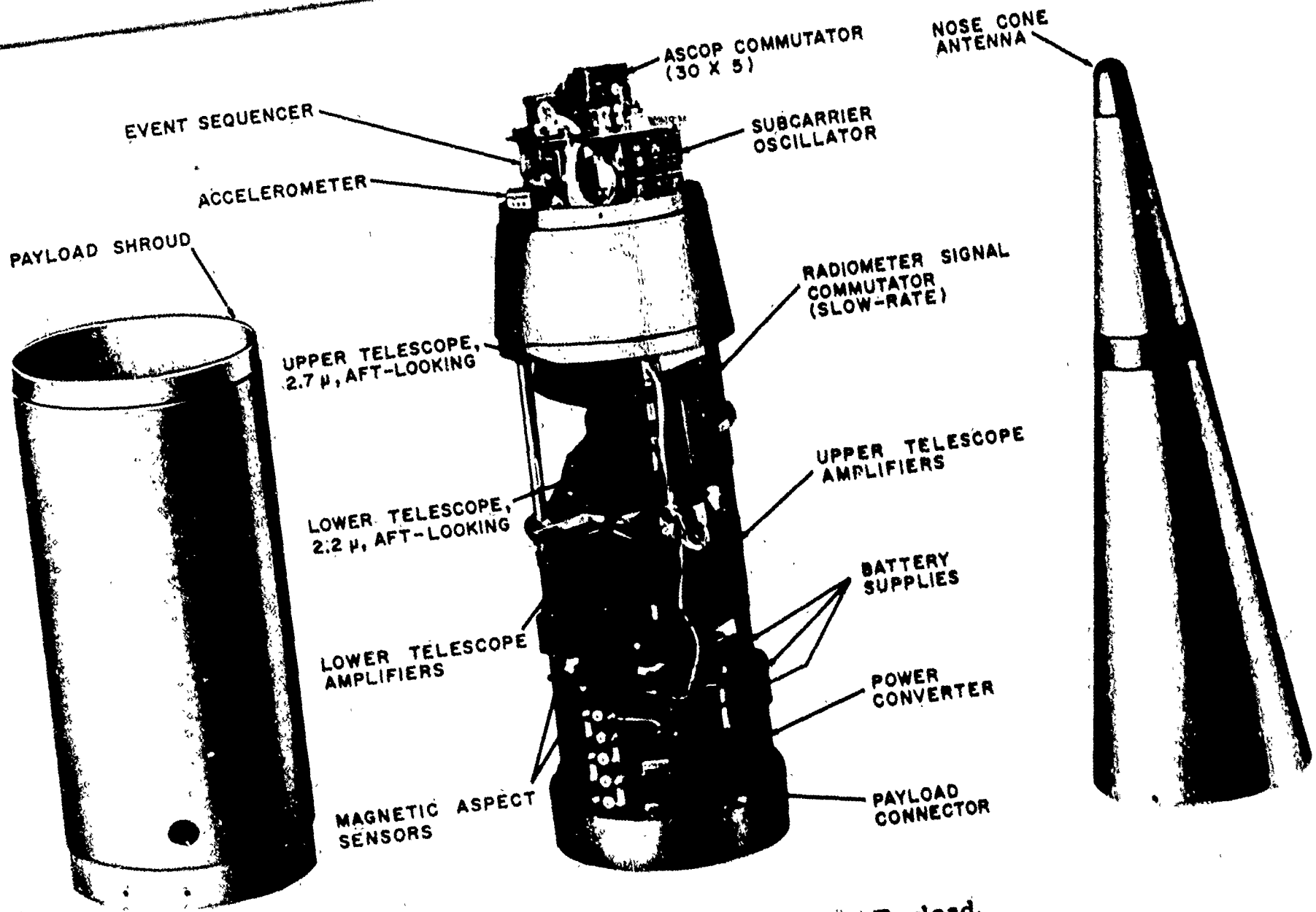

FIG. 9. HITAB-BWSS-02 Payload.

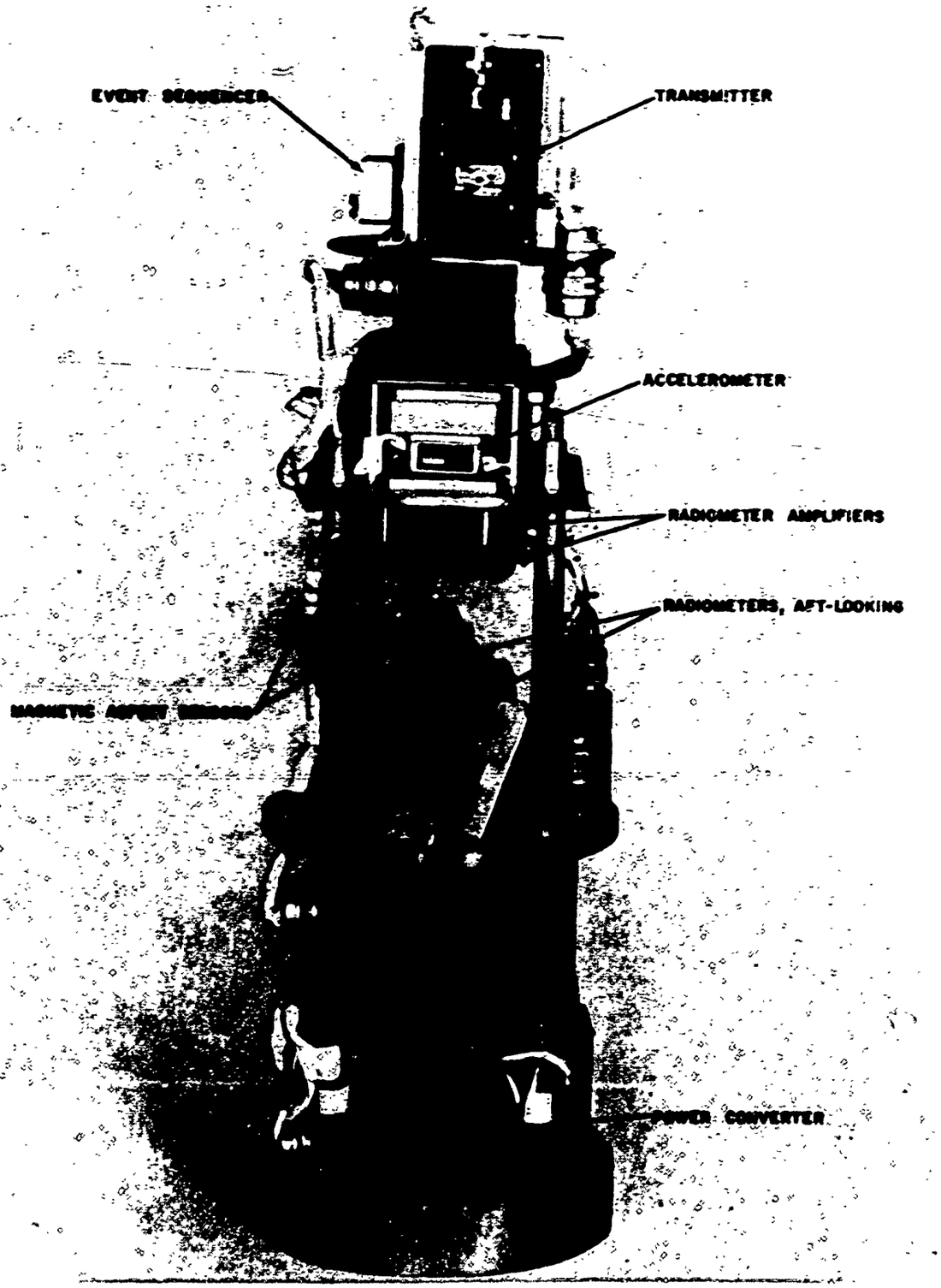

FIG. 10. HITAB-BWSS-03 Payload.

Each payload was fitted with a basic set of equipment (Fig. 9 and 10). The payload contained four general systems: power supplies, data-gathering instrumentation, control equipment, and data-transmission equipment. All payload power was derived from rechargeable batteries of the silver cell or nickel cadmium variety. High voltage power for the telemetry system was derived from the master power supply by a power converter.

Data-gathering instrumentation included the radiometric systems, monitors of optical system and other payload temperatures, voltage supply monitors, a longitudinal accelerometer, and magnetic aspect sensors. The magnetic aspect sensors were installed to provide diagnostic information on the nature of vehicle spin. These units were unidirectionally sensitive, with a dynamic range of ±600 milligauss. One of the sensors was aligned with its sensing axis parallel to the longitudinal axis of the vehicle, while the other was mounted perpendicular to that axis. As long as the spin axis of the vehicle remained coincident with the vehicle longitudinal axis, no modulation would appear on the output of the longitudinal sensor. Simultaneously, the transverse sensor would detect modulation of the magnetic field at the vehicle spin rate (provided the spin axis was not aligned with the magnetic field vector). Therefore, these sensors provided a measure of vehicle spin rate and of perturbations of the spin axis relative to the longitudinal vehicle axis.

Control equipment carried in the payload centered about a combination acceleration switch and timer. The function of this equipment was first to ignite the second-stage motor, and second to eject the payload shroud (Fig. 5). The acceleration switch was tripped by the motion of the vehicle at launching. As this switch was tripped, a timer was started. Nine seconds after launching, the timer applied ignition voltage to the second-stage motor, and 35 seconds after launching, the timer applied a firing voltage to the payload shroud-ejection device. The shroud was simply a thin sheet of aluminum wrapped around the cylindrical portion of the payload. Its purpose was to shield the optics and other payload components from buffeting as the payload rose through the significant atmosphere. The shroud-ejection device was really a retainer that held the wrap-around sheet to the payload. At ejection, the retainer was released, and the shroud followed its natural tendency to spring from the wrap-around condition. The shroud was fitted to the first two payloads, but was omitted from the third because of reliability factors.

Figure 11 presents a block diagram of the data-transmission system as it was initially established for the HITAB-BWSS-03 payload. Modifications were made to this shortly before flight and are discussed later in this report. The block diagrams for the other two payloads differed so slightly from that shown in Fig. 11 that they will not be presented here. Perhaps the most significant feature of the data-transmission

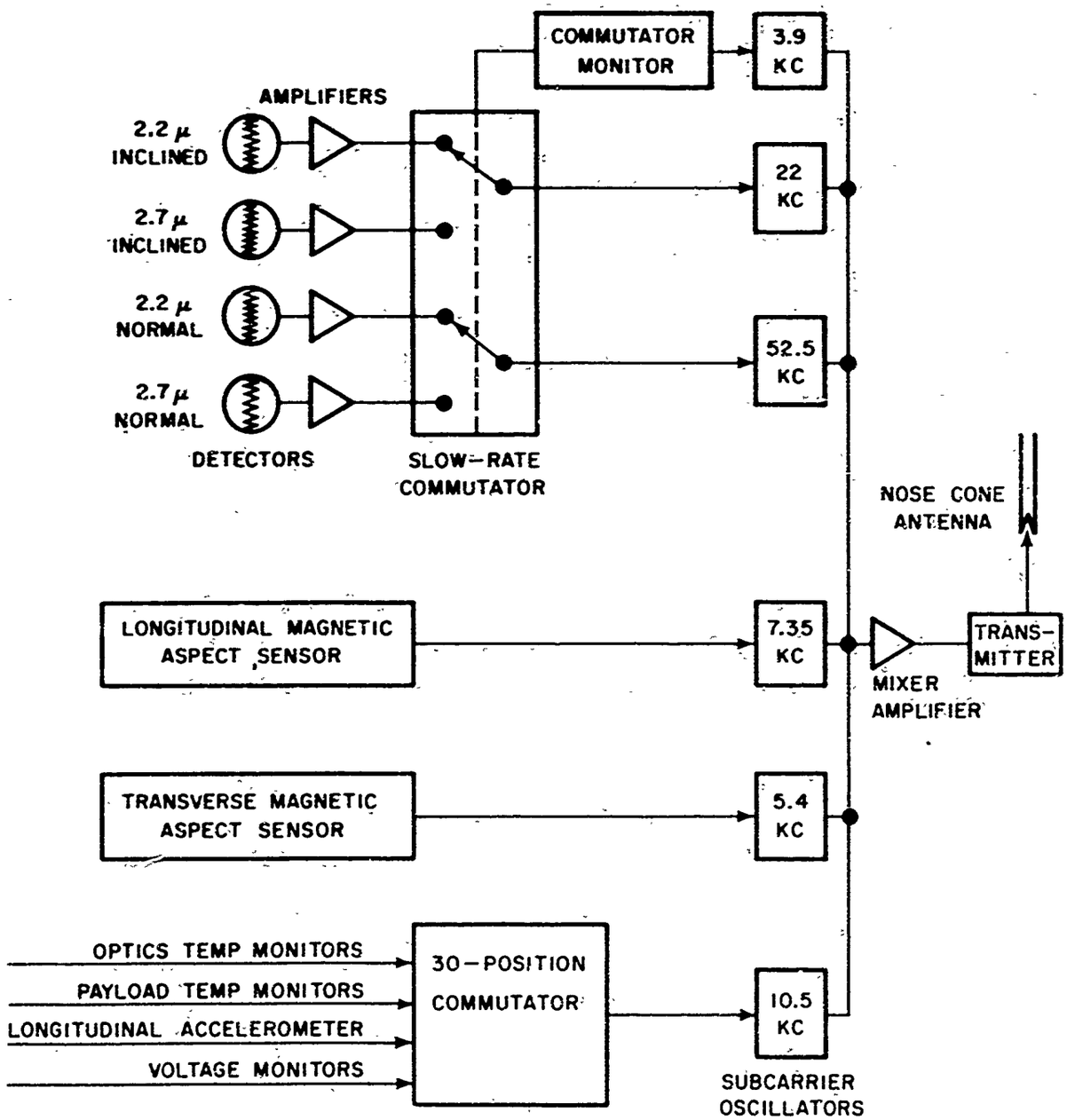

FIG. 11. Data Transmission System Block Diagram.

system is that the data from the two optical systems were subjected to slow-rate commutation. Each of the four radiometric signals (two for each spectral region) were expected to include relatively high information rates. To telemeter these signals then, it was necessary to use the higher frequency subcarrier oscillators available. It would have been preferable to have a separate subcarrier for each channel, but four subcarriers with sufficiently high information bandwidths were not available. The use of a slow-rate commutator seemed to be the most direct solution to this dilemma. The commutator was basically a programmed double-pole, double-throw switch, with the output of each pole fed to a separate high frequency subcarrier. The switch was wired so that the two outputs from each optical system were monitored simultaneously. That is, the output from the 2.2-micron inclined detector was monitored at the same time as the output from the 2.2-micron normal detector. The dwell of the commutator on each pair of outputs was adjusted at roughly 4 seconds, so with a payload spin rate of 2 rps, the outputs of a given system would be observed for 8 payload revolutions.

Ostensibly, an expanded version of this commutation scheme could have been fabricated to allow the time-sharing of the outputs from four optical systems (eight radiometric sensors) on two subcarriers. Such an approach would have satisfied the information bandwidth requirement. This approach was not used because it would have increased the problem of time correlation of signals, and as stated earlier, two additional sets of optics and their associated electronics could not be fitted into the payload.

The remaining three subcarrier oscillators were used to monitor outputs from the two magnetic aspect sensors and from a standard 30-position commutator. This commutator was employed to monitor the outputs of the various voltage and temperature sensors, as well as of the accelerometer.

The payload subcarrier oscillators were frequency-modulated so that their outputs were fixed-amplitude oscillations for which frequency varied in direct proportion to input voltage. The six subcarrier oscillator outputs were combined and amplified by a mixer amplifier, and the resulting composite signal was fed to a frequency-modulated transmitter. The antenna for the system was formed by the external surface of the rocket, with the nose point of the payload fed by the transmitter. This nose point was isolated from the remainder of the vehicle by a micarta block. The antenna was tuned by a matching stub in series with the transmitter and nose point.

IV. OPTICS

As was mentioned earlier, four spectral regions were to be investigated: the 2.2- and 3.8-micron atmospheric windows, and the 2.7- and 4.3-micron atmospheric absorption regions. Commercially available multilayer filters were obtained to define system response within the four bandpasses. These met the following specifications:

Parameter	Bandpass Region			
	2.2 μ	2.7 μ	3.8 μ	4.8 μ
Absolute peak transmission, %	77	58	77	54
Wavelength at peak, μ	2.24	2.733	3.88	4.307
Wavelengths at 50% of peak, μ	2.10 2.42	2.69 2.74	3.630 3.960	4.280 4.340
Wavelengths at 0.1% of peak, μ	1.92 2.70	2.62 2.90	3.24 4.35	4.09 4.57
Bandwidths at 50% points, μ	0.32	0.05	0.330	0.060
Bandwidths at 0.1% points, μ	0.78	0.28	1.11	0.48
Off-band transmission	<0.01%, short of 1.80 μ; <0.03%, 2.80 to 3.50 μ	<0.01%, short of 2.55 μ; <0.03%, 2.95 to 3.79 μ	<0.01%, short of 3.4 μ; <0.01%, 4.4 to 6.85 μ (0.03% at 7.0 μ)	<0.01%, short of 3.95 μ; <0.01%, >4.77 μ;

These filters were fabricated by Optical Coating Laboratories, Inc., Santa Rosa, Calif.

Detectors were also obtained from commercial sources. For operation in the 2.2- and 2.7-micron regions, lead sulfide photoconductive detectors were used. Photoconductive lead selenide units were procured for the 3.8- and 4.3-micron bands. The latter detectors were operated at liquid nitrogen temperature for optimum sensitivity. Figures 12 and 13 are drawings of the lead sulfide and lead selenide detectors. As seen in these figures, the normal and inclined detecting surfaces were deposited on a common substrate. Because differing

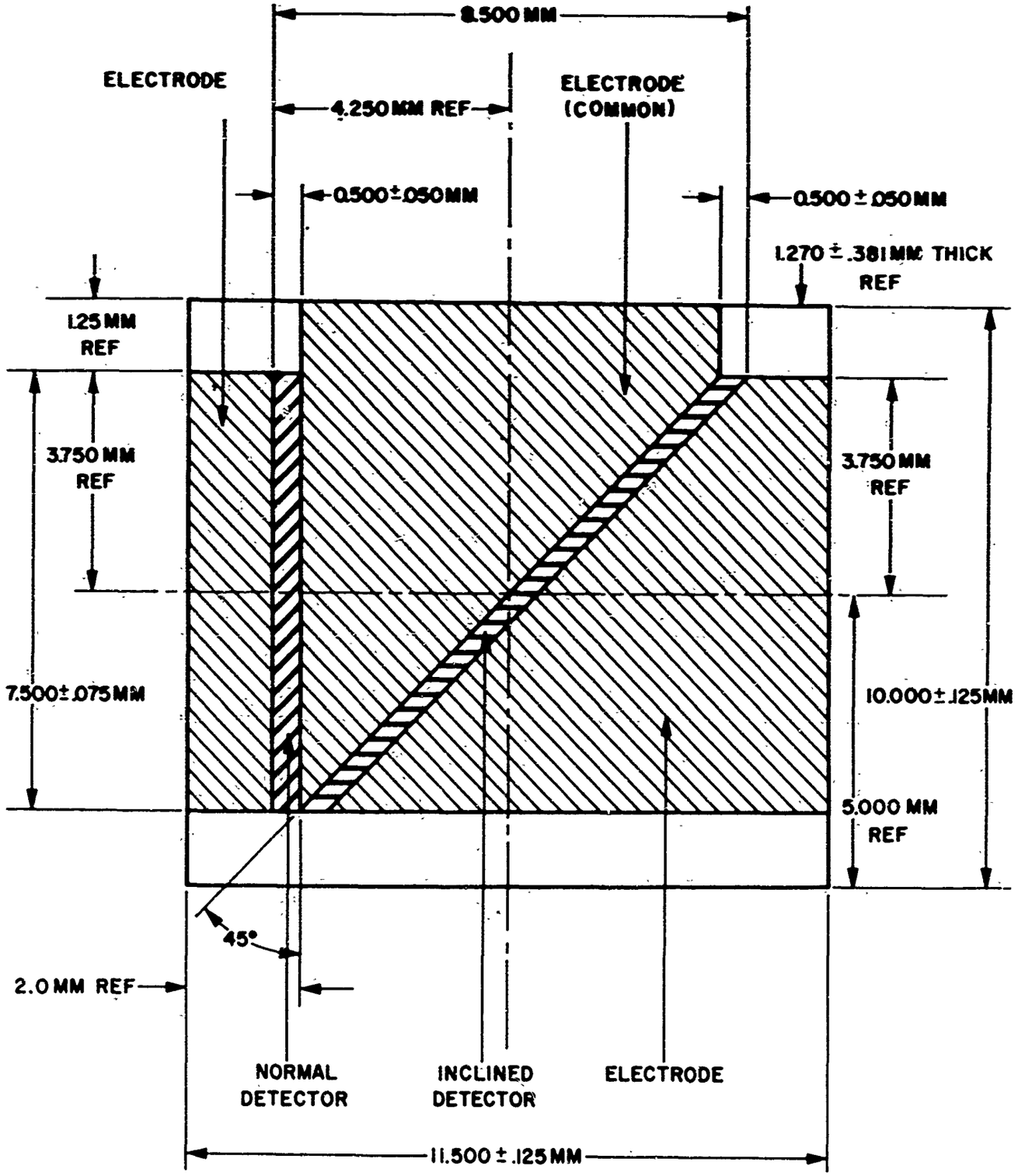

FIG. 12. Two-element Lead Sulfide Detector.

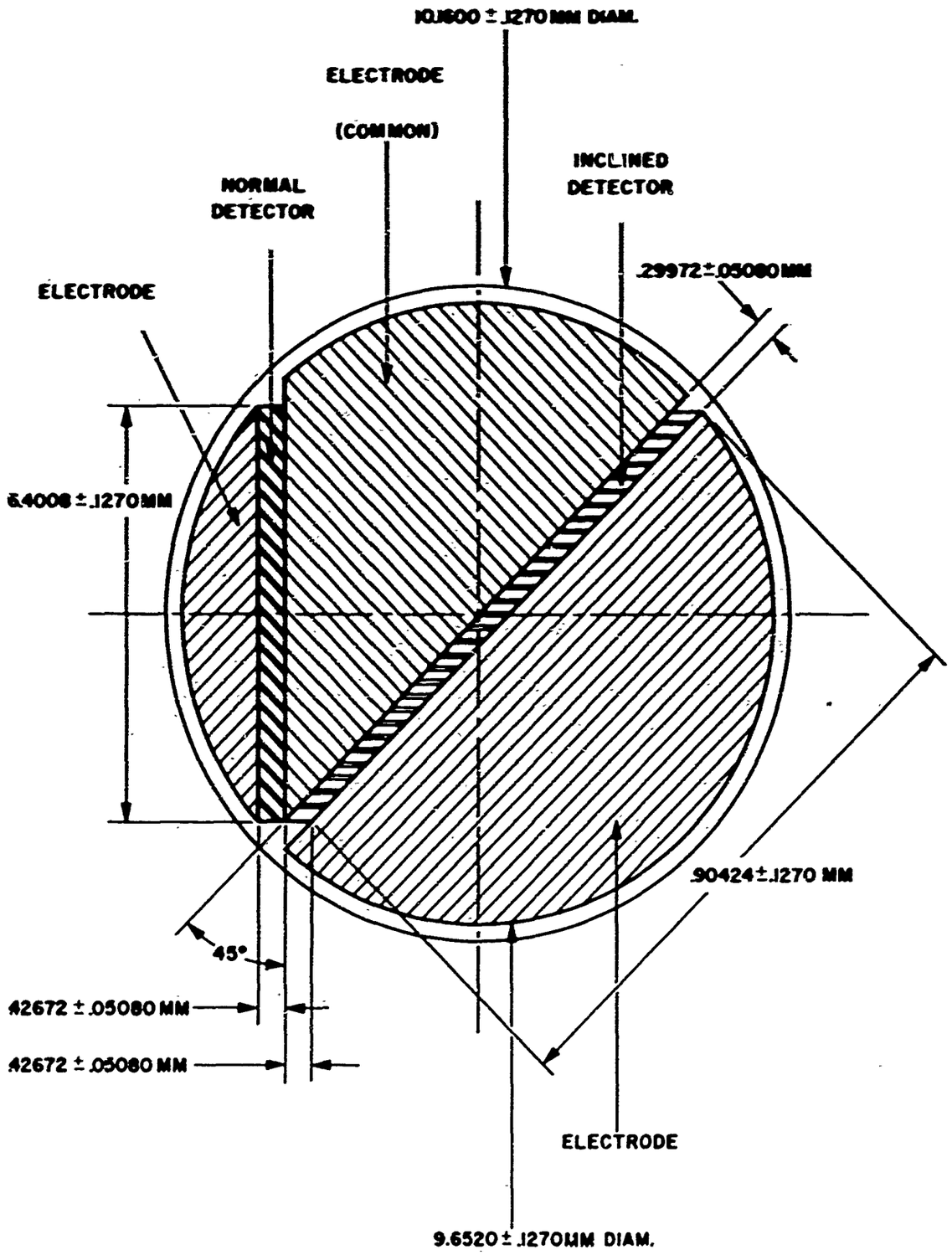

FIG. 13. Two-element Lead Selenide Detector.

sets of optics were used with the two types of detectors, the dimensions of each type varied. However, the aspect ratio (length to width) of the normal detector is 15, and the aspect ratio of the inclined detector is 30 in each case. Note that in the direction of scan (perpendicular to the long side of the normal detector), the widths of the two detector elements are identical.

For the remainder of this discussion, attention will be given only to the optical systems fitted to the three payloads flown. Original intentions were to use 4-inch diameter, f/1 reflective optics with the lead sulfide detectors. This was done for the first two payloads, but in the third, refractive collecting optics were employed. This latter system used a silicon meniscus lens with an entrance aperture diameter of 1.32 inches and a speed of f/1.35 at 2.7 microns. Peak-normalized contour plots were made of the fields of view generated by these two different optical systems. Representative samples of these are presented in Fig. 14 and 15. Figure 14 shows the contour plots for the 2.7-micron system of the -01 payload, and Fig. 15 gives the contour data for the 2.7-micron system of the -03 payload. The information presented in Fig. 14 is typical of the performance of the reflective optical systems used in the first two payloads. Data in Fig. 15 is typical of the refractive systems of the third payload. Specific attention must be paid here to the meaning of "peak-normalized" data. At each elevational position in the view field plots, the 50-percent and 10-percent peak response points are defined in terms of the peak at that elevation. To afford meaning to the data presented in Fig. 14 and 15, it is necessary to refer to Fig. 16 and 17. These two figures plot relative reponse versus elevational position along the peak value trace. Figure 16 contains data for the normal and inclined detector elements of the -01 2.7-micron system, and Fig. 17 presents this data for the -03 2.7-micron system.

Detector signal amplifiers were designed in terms of the information rates expected and the frequency response characteristics of the detectors and telemetry system. Response of the amplifiers constructed was flat within 3 db from 2 cps to 3,000 cps, while the 3-db response limit of the telemetry system was 1,600 cps for the 52.5 kc subcarrier, and 660 cps for the 22-kc subcarrier. Degradation of system frequency response by the amplifiers was small compared with that by the telemetry system. Maximum expected information rates were dependent upon the scan rate and the width of the view field in the scan direction. Nominal view field angular widths for the reflective and refractive optical systems were 5.4 and 11 milliradians, respectively. These values were measured between the 50-percent of peak response points along the direction of scan. For a scan rate of 2 rps, the fundamental information rates would be 1,150 and 570 cps for the reflective and refractive systems. For a scan rate of 4 rps, these values would simply double.

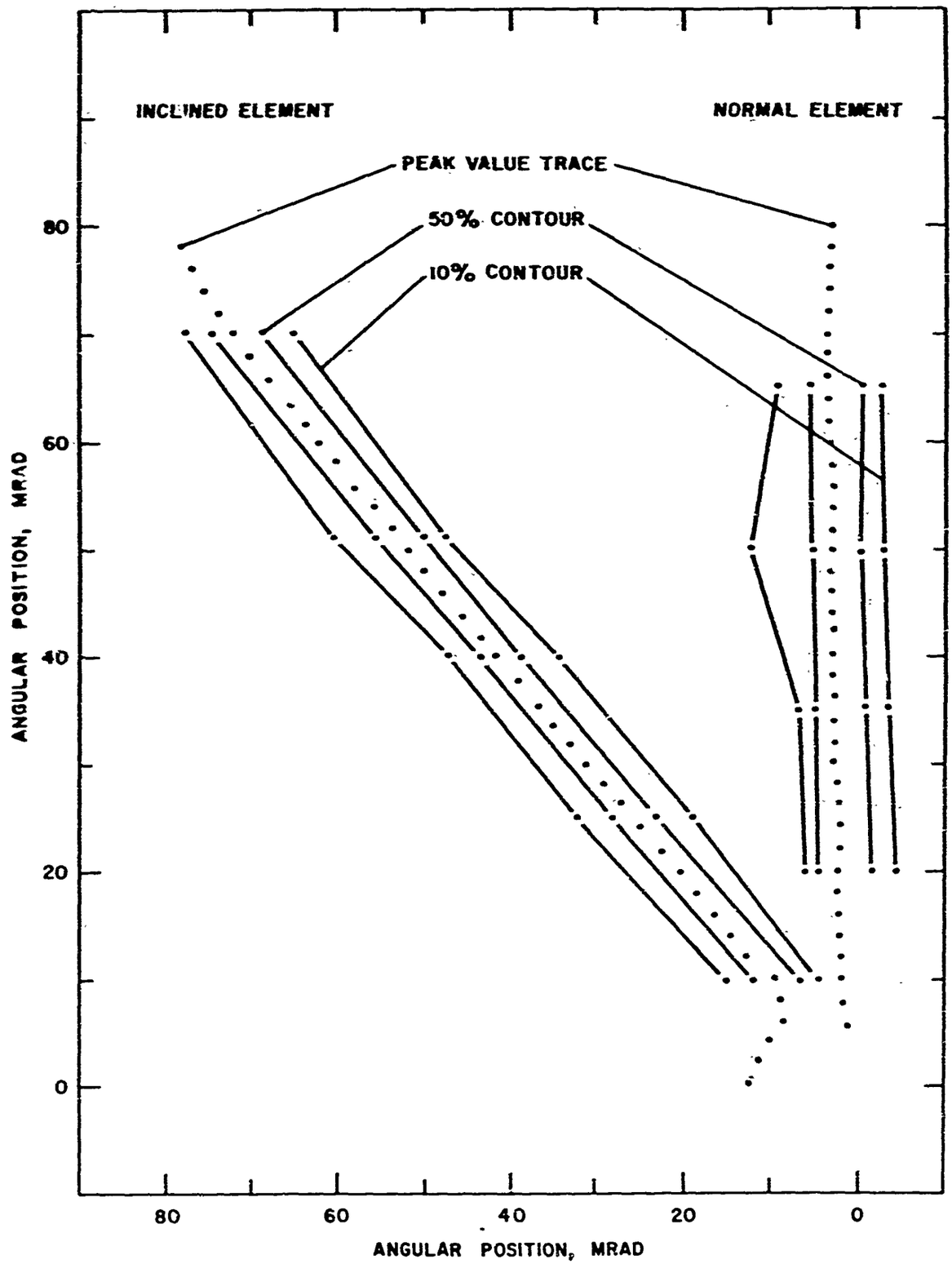

FIG. 14. Field of View Contour Plot, HITAB-BWSS-01, 2.7 Micron System.

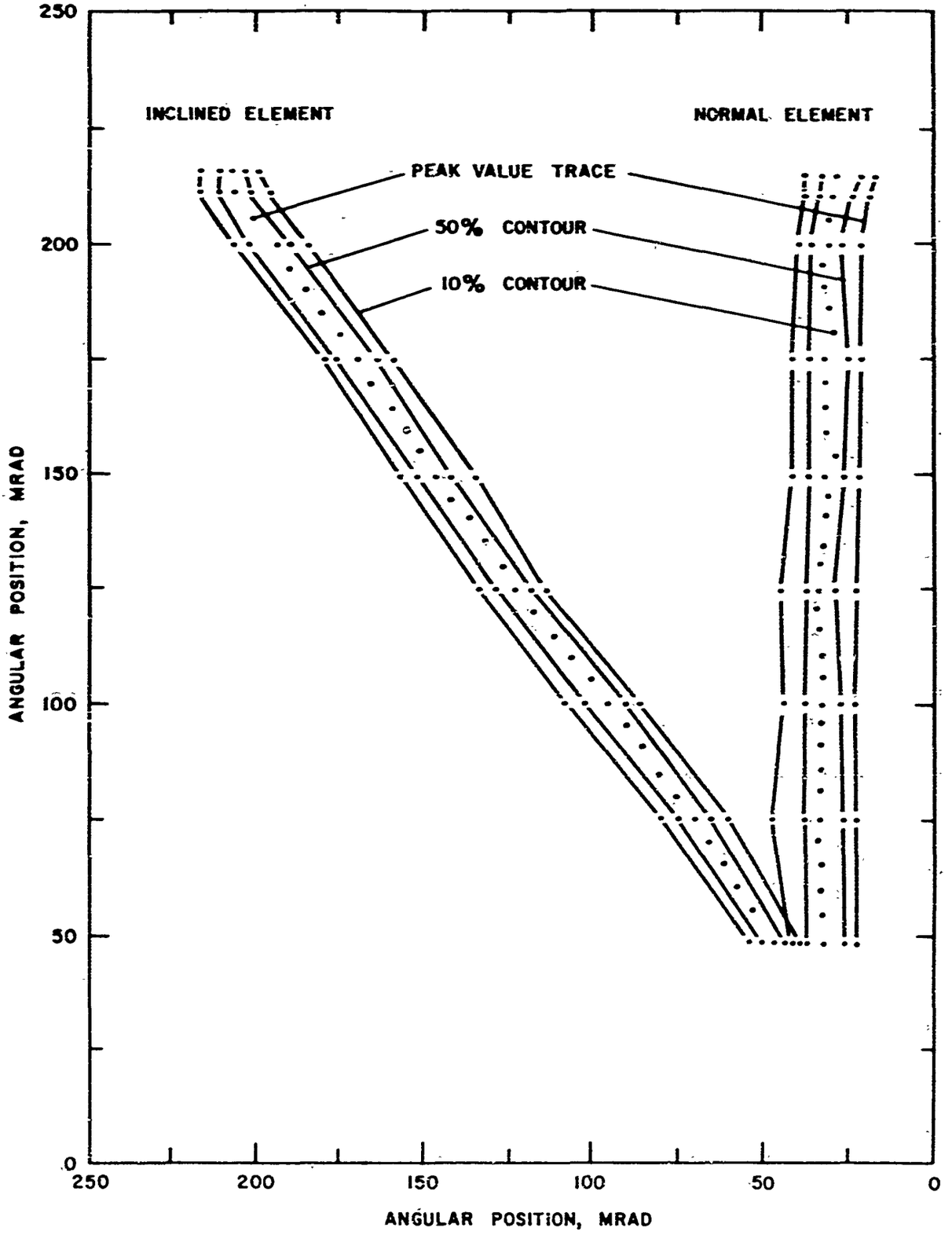

FIG. 15. Field of View Contour Plot, HITAB-BWSS-03, 2.7 Micron System.

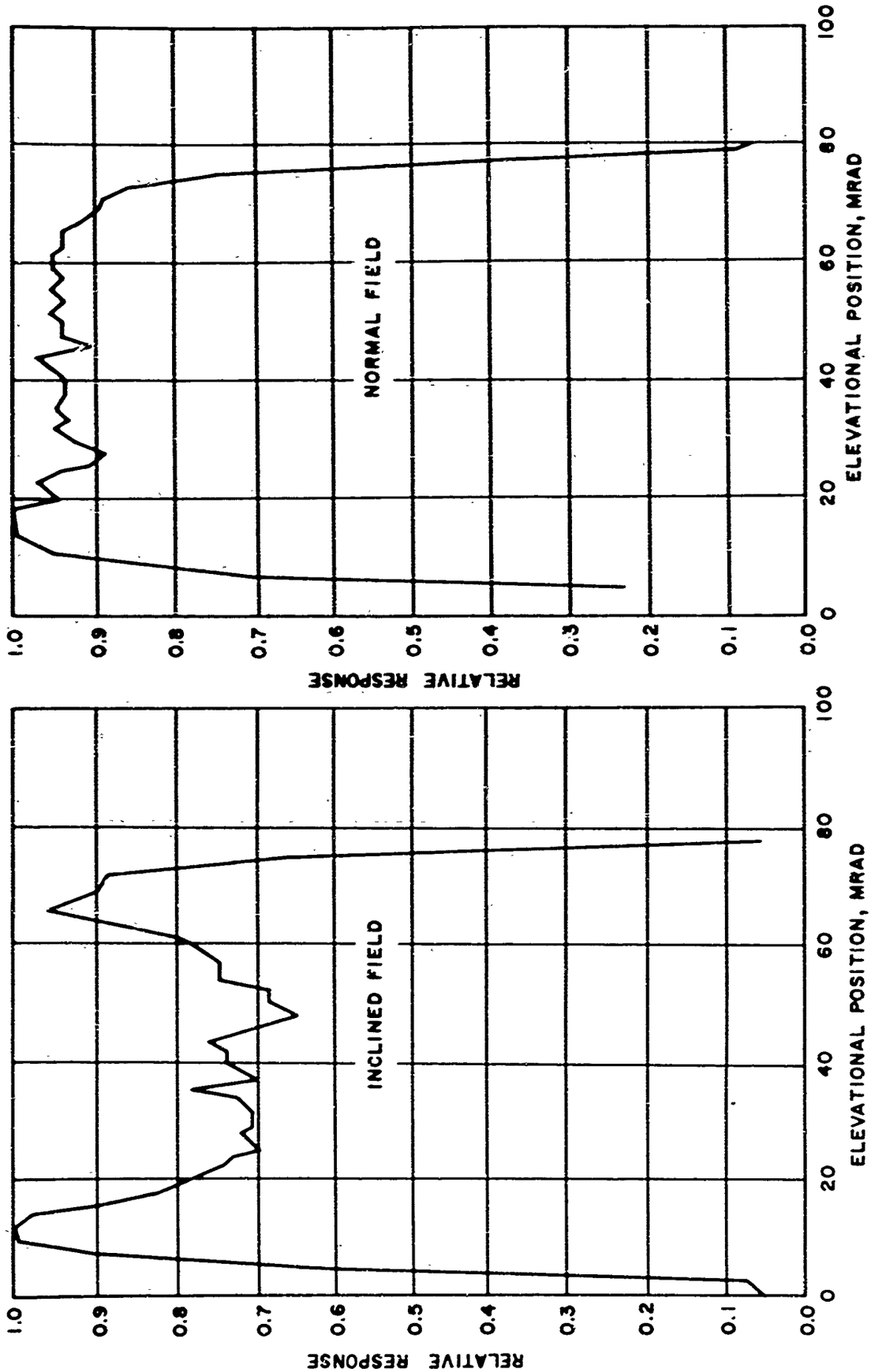

FIG. 16. Relative Response Versus Elevational Field Position, HITAB-BWSS-01, 2.7 Micron System.

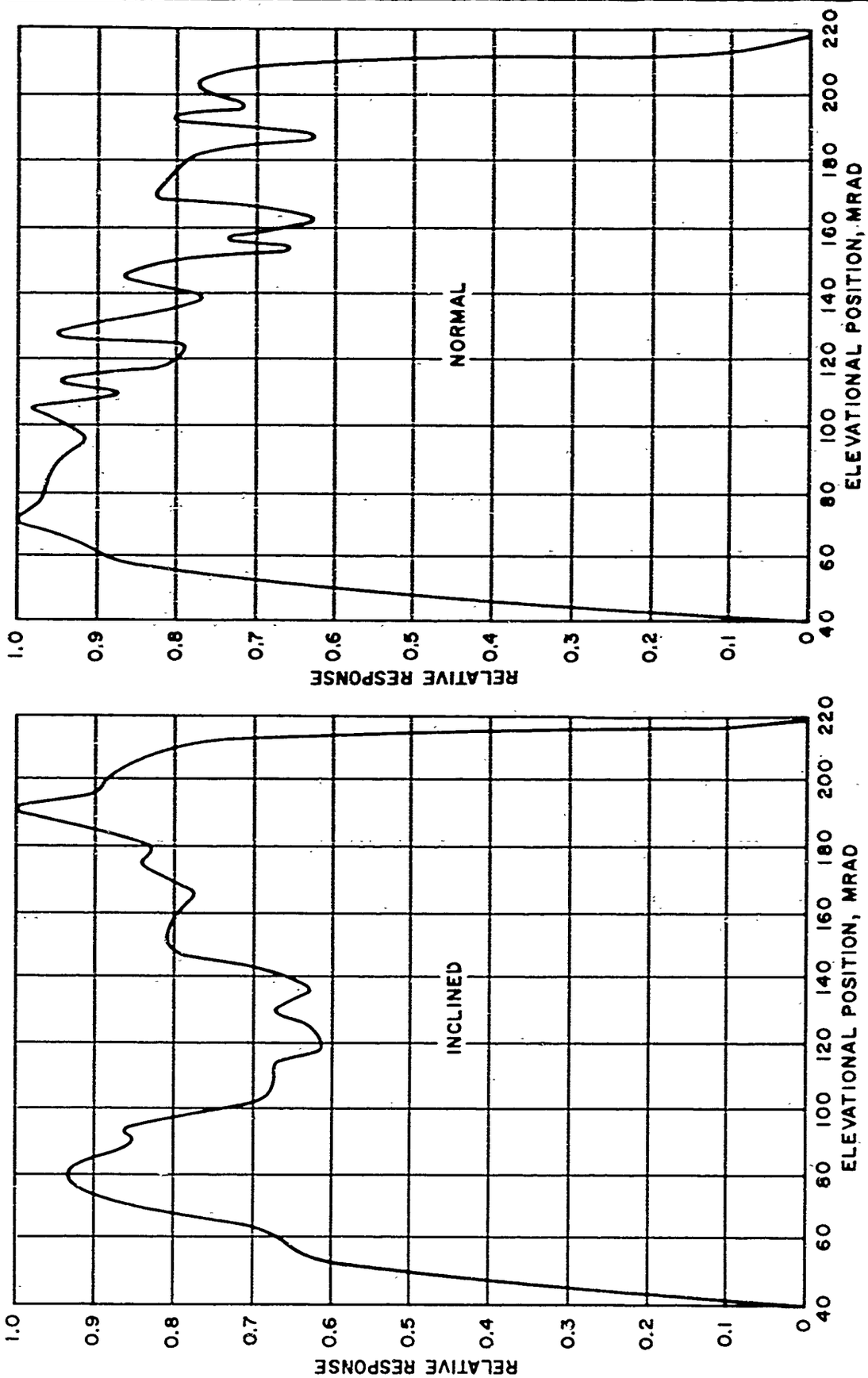

FIG. 17. Relative Response Versus Elevational Field Position, HITAB-BWSS-03, 2.7 Micron System.

A temperature monitoring device was incorporated into each optical system. This device consisted of a thermistor in a voltage divider circuit, which developed an output voltage proportional to the temperature of the monitor. The output of this device was telemetered to give a continuous record of flight-instrument temperature. This voltage was also monitored during instrument calibration to allow direct correlation between calibration and flight data.

V. OPTICAL CALIBRATION

The HITAB-BWSS payloads were not recoverable, thus it was possible to conduct only a preflight calibration of the optical and support systems. The nature of the experiment to be conducted, and the expanse of earth background viewed at any instant established certain conditions for the optical system's calibration. First, it was expected that the instantaneous background viewed by either the normal or the inclined detector would not have a homogeneous, uniformly bright appearance. Second, the frequency content of the system output signals would have the most meaning to the experiment. Third, no zero signal reference level could be obtained during flight, because the radiometer view fields never left the earth.

In accord with these conditions, each system was evaluated primarily in terms of its spectral response, field-of-view, and frequency-response characteristics. The evaluation of system radiance responsivity was placed on a secondary level of importance, as having little meaning in the final data return.

Typical results of the field-of-view evaluations have been presented previously. Nominal transmission characteristics of the filters used in the optical systems have also been presented. The system spectral-response characteristics for the -03 payload optics are presented in Fig. 18. These are representative of the performance of the earlier two payloads' systems.

It is well established that amplifier and detector characteristics are functions of the temperature at which they operate. Since the operating temperatures of the detectors and amplifiers were not controlled in flight, evaluation of the frequency response and radiance responsivity of each system was determined at several instrument temperatures. The range of these was chosen to bracket those temperatures expected in flight. Data were taken at four instrument temperatures, approximately evenly spaced, between 10 and 65°C.

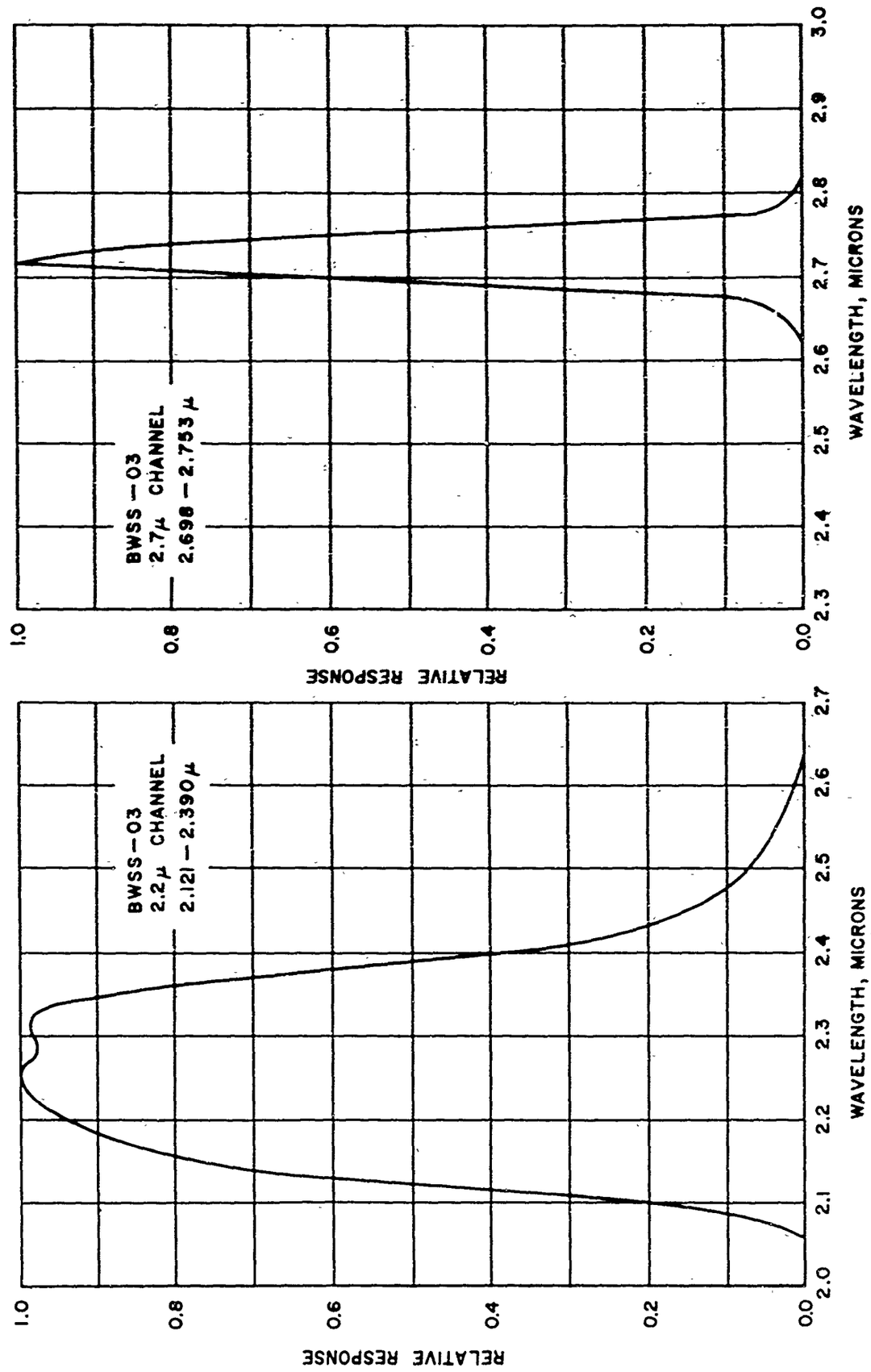

FIG. 18. System Spectral Response, HITAB-BWSS-03, 2.2 and 2.7 Micron Systems.

System frequency response and radiance responsivity calibrations were conducted simultaneously. A specially constructed environmental chamber was employed to simulate the flight-temperature environment, (Fig. 19). The chamber cavity could accommodate the entire BWSS or HITAB-TRIS[8] payload (the TRIS payload is shown under test in Fig. 19).

Cavity temperature was controlled to ±3° C following a half-hour stabilization period. The mounting pedestal in the chamber had 3 degrees of translational and 2 degrees of rotational freedom. A circular port in the side of the chamber was fitted with a flange that provided a sealed connection between the chamber and the external calibration source. The source consisted of an off-axis parabolic mirror, a folding mirror, and the radiation source (defined by a circular aperture). By placing the radiation source at the focal point of the parabolic mirror, it was effectively removed to infinity when viewed from the chamber. The folding mirror simply rotated the focal point of the parabolic mirror to the side of the collimator to facilitate mounting the source. Air fittings were provided to allow the atmosphere of the chamber to be purged with high purity air, free of water and carbon dioxide vapor. Absorption of radiation by these constituents was controlled to the point that it would not degrade the calibration.

It was desirable to subject the entire BWSS payload to environmental control. However, the radiometer optical axes were aligned 30 degrees off the payload longitudinal axis. The chamber pedestal could not tolerate the loads induced by tilting the payload 60 degrees, allowing for proper radiometer alignment with the collimated radiation beam. Hence, the radiometer-amplifier of interest was removed from the payload and directly mounted on the pedestal. The remainder of the payload was not environmentally controlled during calibration. It was felt that this would not seriously degrade the quality of the calibration since the detector and amplifier were the prime contributors to temperature dependence.

Because modulation of radiant signals in flight was to be achieved through payload spin (object space modulation), modulation of calibration source radiation was necessarily induced by a chopping system. This was fitted between the radiation source and the source aperture. The chopper wheel had a 50-percent duty cycle, and was driven by a controller system that maintained the chopping frequency within ±1-percent of the given rate. Source apertures were selected by manually rotating the aperture selector wheel. The aperture wheel lay between

[8] U. S. Naval Ordnance Test Station. HITAB-TRIS Payload, by James E. Hurtt, Ray N. Francis, and Larry N. Pace. China Lake, Calif., NOTS, June 1964. (NAVWEPS 8503, NOTS TP 3480).

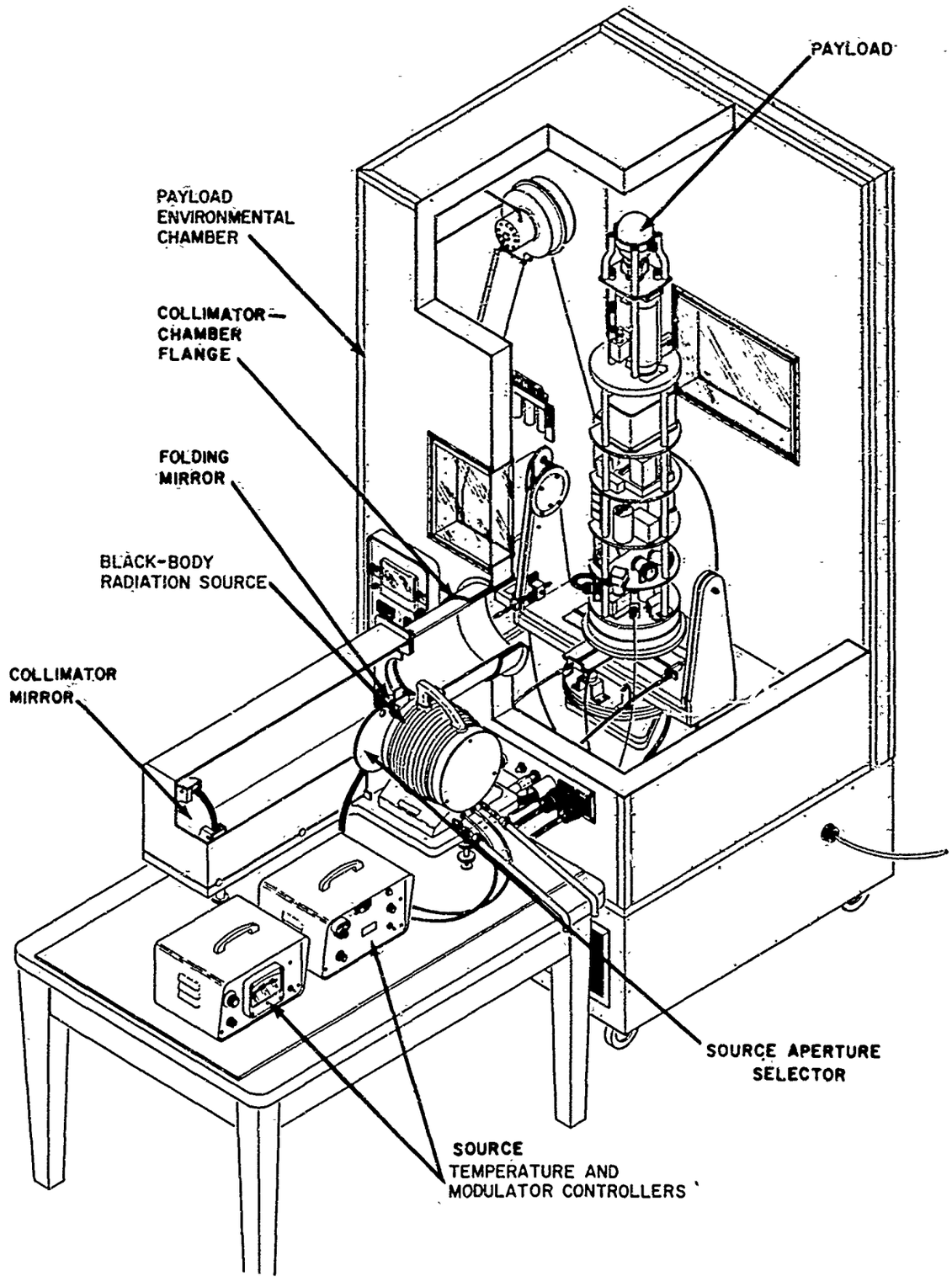

FIG. 19. Calibration Chamber.

the chopping wheel and the collimator system. Radiant emission of the source followed the classical black-body characteristic, with an emissivity of 99 ± 1-percent. The emitting surface of the source was a graphite cone, and the temperature of the source was determined by a thermocouple placed within the cavity of the source. The necessary emission characteristics of the source were calculated from the Planck radiation function.

To evaluate the frequency response of a given system, the payload was oriented in the chamber so that the optic axis of the radiometer being calibrated was aligned with the optic axis of the collimator. The temperature of the radiation source was adjusted to a value for which the output of the system (at its peak frequency-response point) was close to the maximum allowed. The output of the optical system was then recorded on magnetic tape (through the telemetry system of the payload), as a function of chopper frequency. Oscillograph chart records were made of the tape-recorded signals, and output versus frequency was read. This process was carried out at each instrument calibration temperature.

As mentioned in the section on optical systems, each system was fitted with a temperature monitor, which developed an output voltage proportional to temperature. The output of this unit was recorded both in flight and in calibration, so that direct correlation between calibration information and flight data was possible. Frequency-response plots of the 2.2- and 2.7-micron inclined and normal optics of the BWSS-03 payload are shown in Fig. 20 and 21. These are system characteristics, showing the combined effects of detector, amplifier, and telemetry response. Recalling that the inclined detector outputs are impressed on the 22-kc subcarrier (660 cps response), and that the normally positioned detector outputs are impressed upon the 52.5-kc subcarrier (1,600 cps response), note that the inclined optics response rolls off much faster than does that of the normally positioned optics. The characteristics shown here are representative of the performance of the earlier two payloads.

Radiance responsivity calibration was carried out in much the same fashion. In this case, the chopping frequency was fixed at a convenient value within the flat portion of the frequency response. The output of the radiometer under test was recorded as a function of input radiation level. Because of the angular size of the optical view fields and the geometry of the radiation source collimator, it was not possible to flood the radiometer fields of view. For this reason, the calibration was made in terms of aperture irradiance. In order to convert this to a radiance calibration, it was necessary to know the exact placement of the source image in the view field. Then, given the contour plots of the view field, the solid angle view field could be determined, and direct conversion to equivalent radiance was possible.

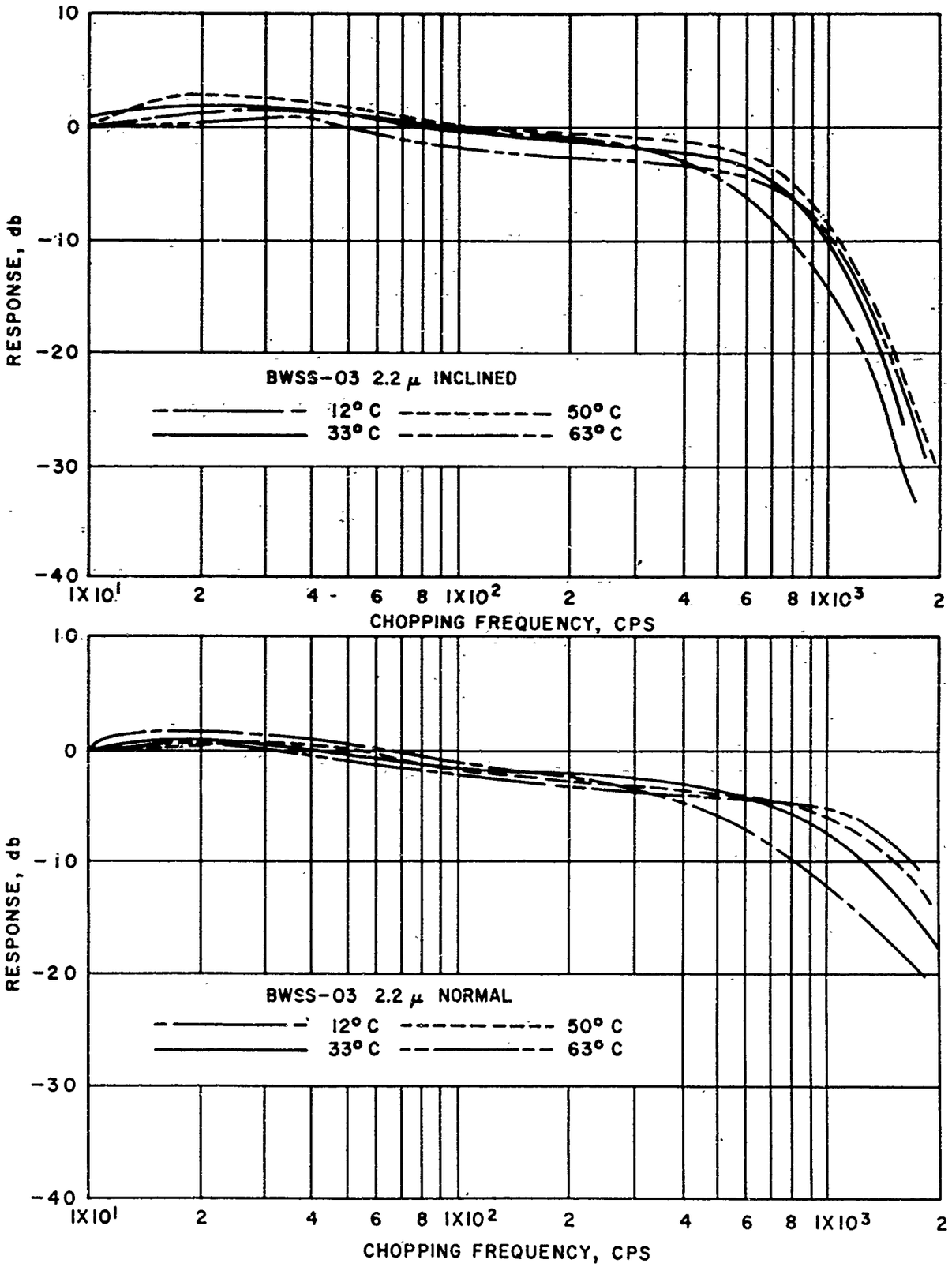

FIG. 20. Frequency Response Characteristics, HITAB-BWSS-02, 2.2 Micron System.

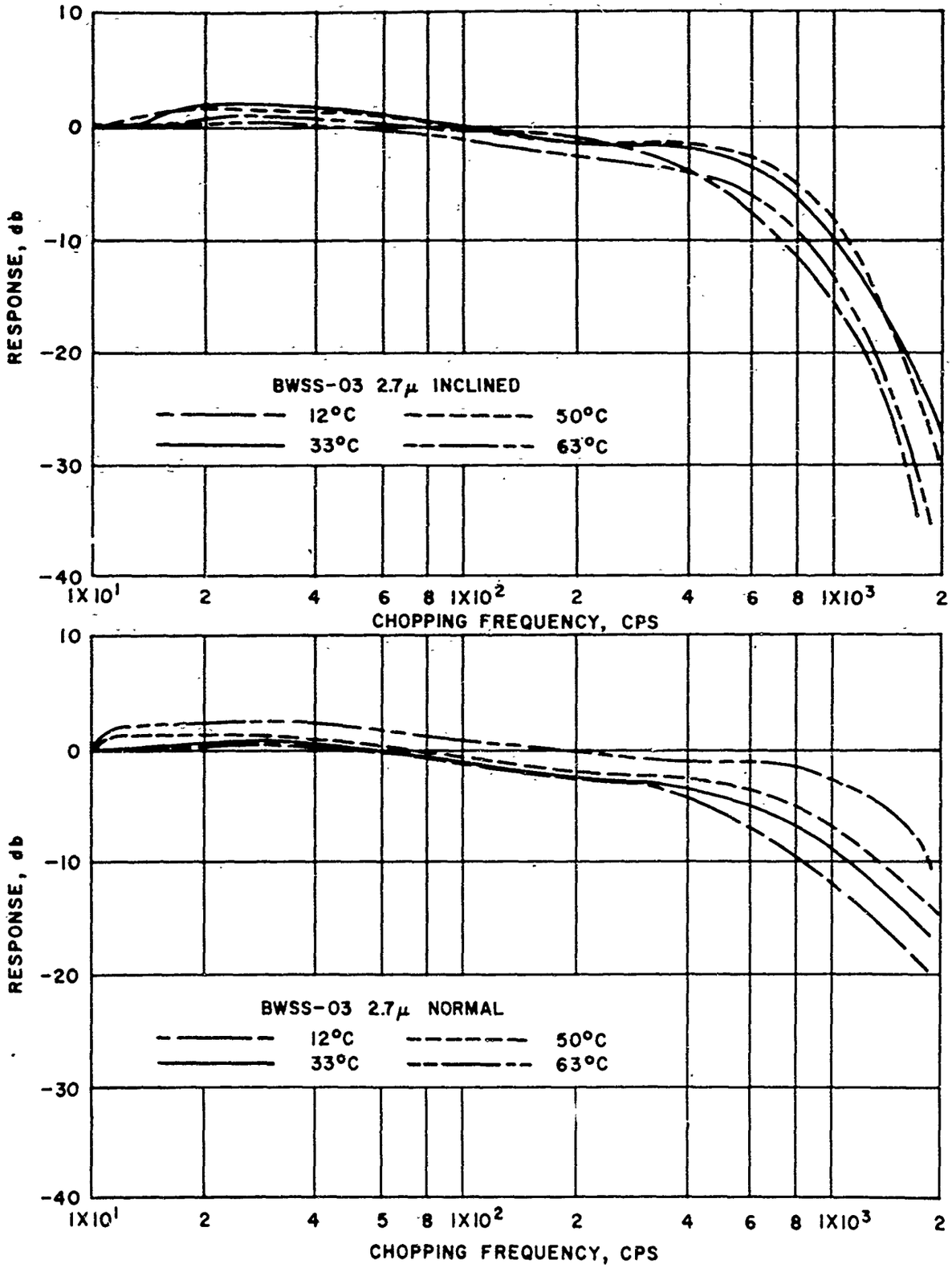

FIG. 21. Frequency Response Characteristics, HITAB-BWSS-03, 2.7 Micron System.

Input radiation levels were chosen to span the dynamic range of each optical system, and were obtained by varying the source temperature, source aperture size, and by using neutral density attenuation filters at the source. These filters were inserted between the radiation source and chopping wheel, and had relatively constant (known) transmission over the range of 1 to 6 microns. A series of these was available, having transmission at selected levels between 10 and 70-percent absolute transmission. Typical results of the radiance responsivity calibration are presented in Fig. 22 and 23. Data for the 2.2-micron system from the -03 payload are shown in Fig. 22, and the 2.7-micron system data from the same payload are shown in Fig. 23. Here, radiance at the center wavelength of each spectral passband is plotted as a function of radiometer output voltage for each of the four instrument calibration temperatures. Also noted on these figures are the output voltages of the temperature monitors to which each trace corresponds. In applying the responsivity calibration data to the raw field data obtained by the optical systems, the monitor output voltages were used as the means of correlation.

VII. RESUMÉ OF ROCKET FLIGHTS

All three HITAB-BWSS payloads were launched from the Gulf Test Range, Eglin Air Force Base, Florida. HITAB-BWSS-01 was launched on 19 February 1962. Telemetry signals from this payload were abruptly terminated 10 seconds after launching, but the data obtained prior to that time indicated probable destruction of the vehicle during second-stage motor burning.

HITAB-BWSS-02 was launched on 23 June 1962. Telemetry from this payload became intermittent 15 seconds after launching, and the tracking antennas failed to monitor the telemetry after this time. No radar data were obtained on either this or the previous shot.

HITAB-BWSS-03 was launched on 27 November 1963. Telemetry was received from launching to 120 seconds later, and the signals obtained appeared to be of good quality. Ground-based radars were able to track the vehicle from summit to shortly before impact. Some last minute modifications were made to the data transmission system for this payload. Shortly before launching, the 30-position commutator used for transmission of support instrumentation data was found to be excessively noisy. It was decided that the commutator should be bypassed, so it and the longitudinal aspect sensor were deleted from the data system. The two optical system temperature monitors were then impressed upon the two vacated subcarrier oscillators. The remaining telemetry assignments were unchanged.

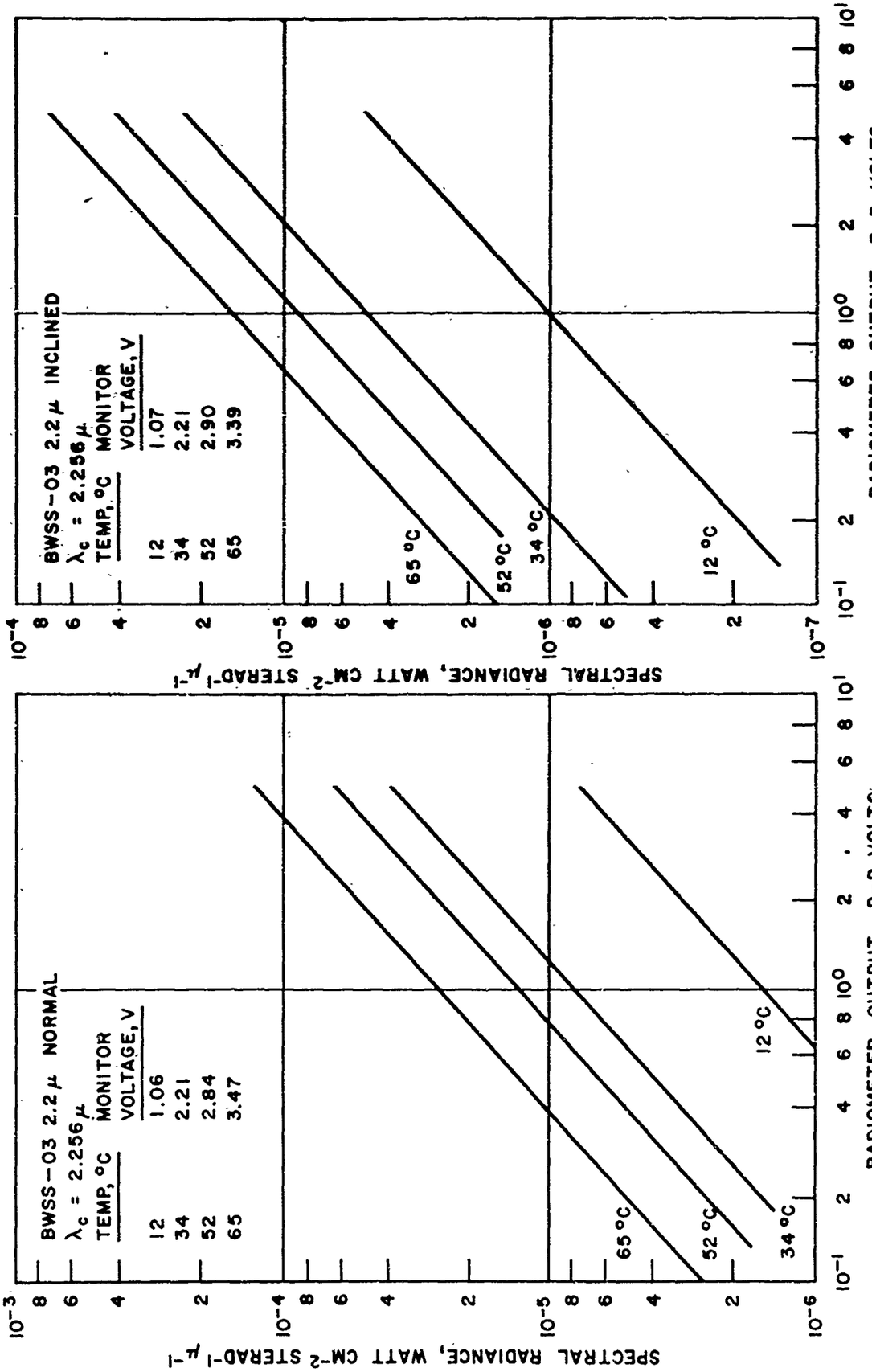

FIG. 22. Radiance Response Characteristics, HITAB-BWSS-03, 2.2 Micron System.

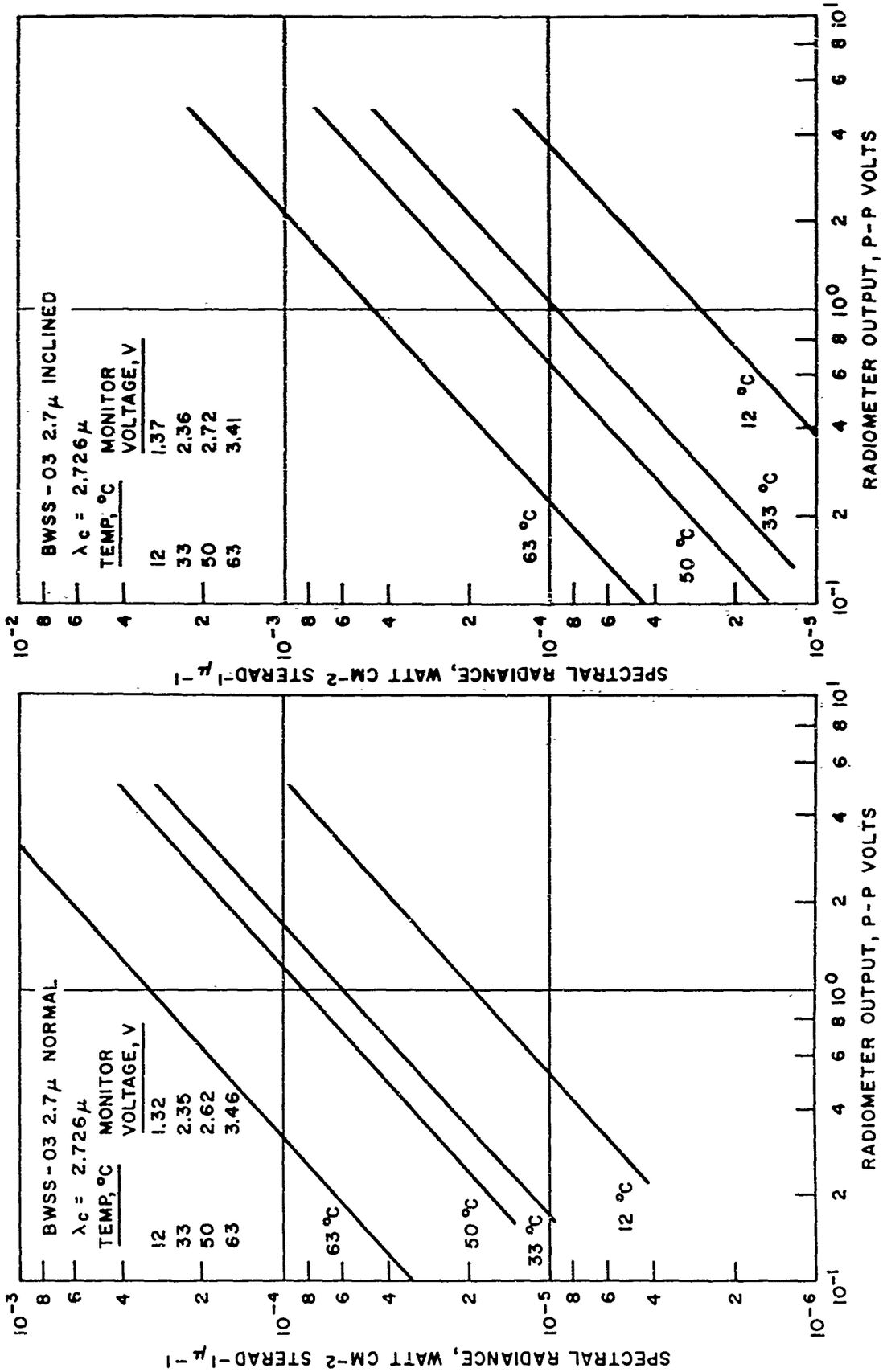

FIG. 23. Radiance Response Characteristics, HITAB-BWSS-03; 2.7 Micron System.

The spin rate attained by the -03 payload was 9 rps, which netted a fundamental maximum information rate of approximately 2,500 cps. This rate exceeds the information bandwidth of the telemetry system (1,600 cps on the 52.5-kc subcarrier and 660 cps on the 22-kc subcarrier). Given the frequency response data for the optical systems involved, it should be possible to correct for the degradation that is due to the high spin rate.

Figure 24 is a copy of a portion of the oscillograph chart record made of the BWSS-03 flight telemetry record. It is clear that the 2.2-micron channels were saturated during a part of each payload revolution, but a fair amount of nonsaturated, high frequency modulation was present in its waveform. The 2.7-micron channels, on the other hand, never saturated, and the structure of the signals seems to be generally characterized by lower frequencies.

Cloud conditions for the -03 flight were as follows. A layer of stratocumulus clouds, with a base at 0.2 km and a top at 1.2 km extended over the area inland from the launching point. Offshore winds maintained a fairly abrupt edge to this layer 16 km inland, which roughly paralleled the Gulf coast. Coverage of this layer was 80 to 100 percent. The area surrounding the launching point was overcast with altocumulus clouds of a mean altitude of 7.6 km and a thickness of 0.6 km. The degree of coverage was 20 percent. A 60-percent buildup of fluffy cirrus extended to 10 km in the area 64 km north and 32 km east of the launching point. This buildup extended in altitude from 8.5 to 10 km. Another 60-percent buildup of cirrus extended to 10 km in the area 80 km north and 40 km west of the launching point. Cirrus coverage generally increased to the south and southwest of the launching point.

VIII. SUMMARY AND CONCLUSIONS

The vehicle employed in the HITAB-BWSS sounding rockets was used extensively with other HITAB payloads, as well as in other projects. Failure of the first of the BWSS series of rockets occurred early in the employment of the Terrier-Viper combination. Problems with igniters and other critical items have been overcome, and the vehicle stands as a useful sounding-rocket system.

While the third payload in the HITAB-BWSS series successfully generated Wiener spectra of the earth's infrared background, there are certain improvements that seem to be in order if such measurements are to be made in the future.

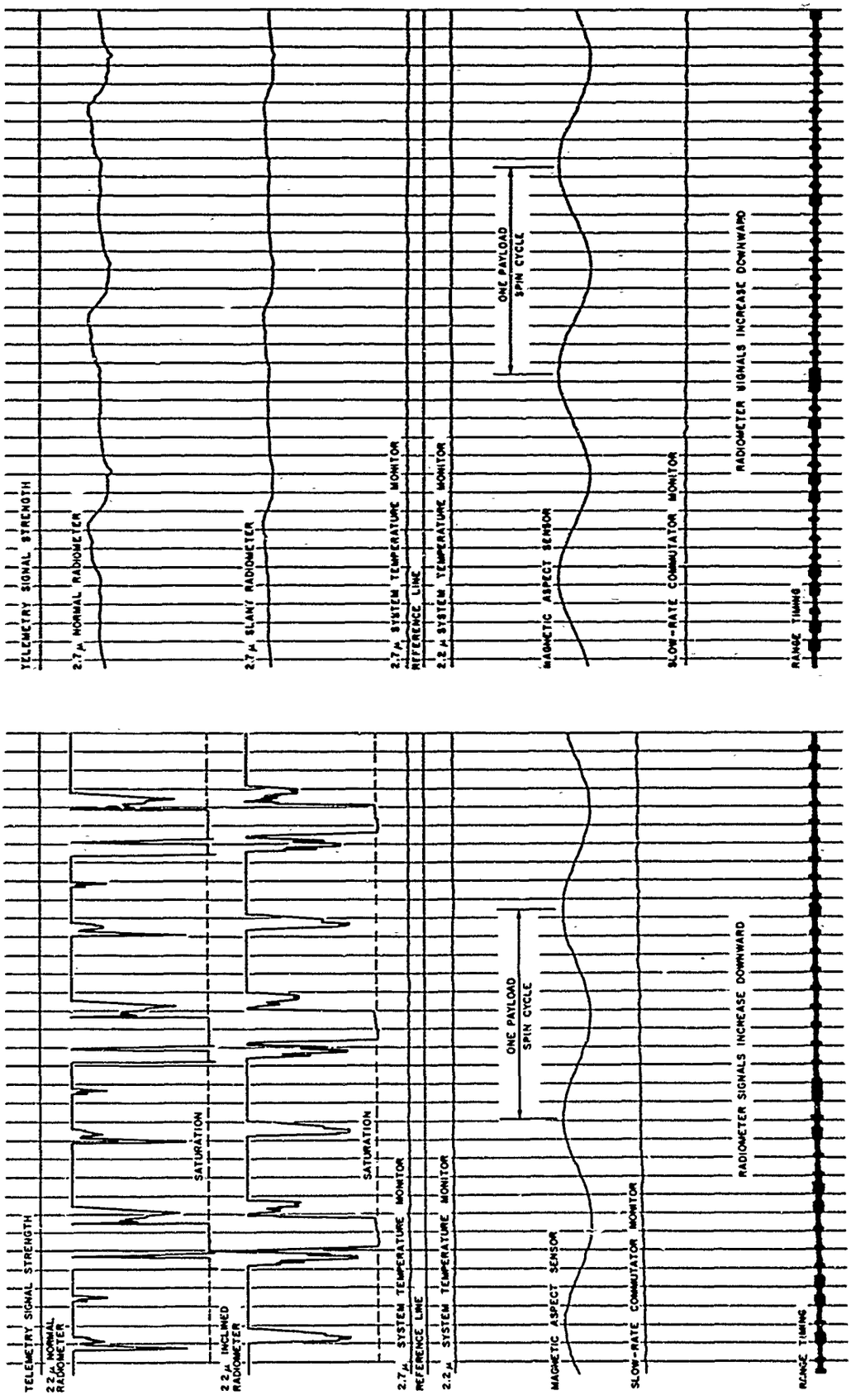

a. T + 105 Seconds.

b. T + 110 Seconds.

FIG. 24. Segments of HITAB-BWSS-03 Flight Record.

First, strong consideration should be given to the use of some form of vehicular attitude control. With the system employed, it was not possible to establish accurately the space orientation of the payload airframe. Thus, an accurate statement of the nature of the scan and the projected shape of the view field in object space could not be made.

Second, a different form of scan should be employed. The spiral approach is convenient because it allows knowledge of the cloud cover over the entire area scanned. Object space was sufficiently limited that aircraft reconnaissance of the cloud cover provided a highly detailed accounting of the entire zone. The spiral technique also gives redundant scanning—there is a great deal of overlap between background coverage of successive scans. However, the spiral approach requires the radiometer optic axes to be tilted with respect to the payload spin axis. Unless this tilt angle can be minimized, the projected shape of the view field in object space becomes decidedly trapezoidal. This reduces the spatial resolution of the measurement. Use of a shallow-arc trajectory and a line scan would overcome the problem of view-field distortion, but would require reconnaissance of a much larger object space. The line-scan method would add the feature of increased background area coverage. It would thus allow the monitoring of many different background distributions in a single flight. The advantages of this approach appear to outweigh its disadvantages.

Third, the view fields of the radiometers should have uniform response over their limits. This could be accomplished by the use of fiber optics or light piping, which would have a rectangular cross section at one end, and a circular cross section at the other. Integration effects achieved by this system would produce a more uniform field, and would allow the use of less expensive, more reliable detectors. Cost of the necessary optics could be significant, but they would allow selection of even higher aspect ratios than could be obtained in the case of detector-limited view fields.

Fourth, in order to reduce the uncertainty inherent in extrapolating from one-dimensional to two-dimensional data, additional inclined elements could be incorporated. These would be oriented at various angles to the scan direction, and would provide more data points from which to construct the necessary extrapolation.

Fifth, it would be desirable to have continuous data coverage for each radiometric channel. This would require a more sophisticated data recovery system, but would allow true correlation between the data obtained for each spectral region investigated.

It has not been the intent of this report to show that the two-dimensional Wiener spectrum is the best means for characterizing backgrounds. This report has shown that there are two serious drawbacks associated with the inclined view-field approach to two-dimensional Wiener spectrum measurements. First, it is practically impossible to produce a long, narrow, detector-limited view field with uniform response over its limits. Second, the extrapolation required to obtain the Wiener spectrum along the second spatial direction is so coarse that data so generated are highly questionable. The inclined view-field system will generate meaningful one-dimensional data—one must seriously question the quality of two-dimensional data obtained by extrapolation.

ACKNOWLEDGEMENTS

The authors wish to acknowledge the sponsorship, support, and advice of Ralph Zirkind of the Optics Branch, BMD, Advanced Research Projects Agency (ARPA). Project engineering and range coordination was provided by Kenneth Vickery and Marshall Cartledge, Code PGWHP, Eglin Air Force Base, Florida. Data analysis support is being supplied by the Institute of Science and Technology (IST), University of Michigan.

Layout, construction, wiring, and checkout of the BWSS-01 and -02 payloads was done by Alvin B. Cles and Robert G. Crawford of the Astrometrics Division, USNOTS, China Lake, California. Layout and Construction of the third payload was done under a service contract, by Minneapolis-Honeywell, Inc., at their Duarte, California, plant. Advice on the physical characteristics of the optical view fields was rendered by Lucien M. Biberman of the Institute of Defense Analysis (IDA). George A. Wilkins of the Astrometrics Division, USHOTS provided assistance in the specifications of the optical systems.